Available online at www.sciencedirect.com
ScienceDirect
Computer Physics Communications 178 (2008) 301–330
Computer Physics Communications
www.elsevier.com/locate/cpc

POTHMF: A program for computing potential curves and matrix elements of the coupled adiabatic radial equations for a hydrogen-like atom in a homogeneous magnetic field ☆

O. Chuluunbaatar [a,*], A.A. Gusev [a], V.P. Gerdt [a], V.A. Rostovtsev [a], S.I. Vinitsky [a], A.G. Abrashkevich [b], M.S. Kaschiev [c], V.V. Serov [d]

[a] *Joint Institute for Nuclear Research, Dubna, 141980 Moscow region, Russia*
[b] *IBM Toronto Lab, 8200 Warden Avenue, Markham, ON L6G 1C7, Canada*
[c] *Institute of Mathematics and Informatics, Sofia, Bulgaria*
[d] *Saratov State University, Saratov 410012, Russia*

Received 16 April 2007; received in revised form 17 September 2007; accepted 21 September 2007

Available online 29 September 2007

Abstract

A FORTRAN 77 program is presented which calculates with the relative machine precision potential curves and matrix elements of the coupled adiabatic radial equations for a hydrogen-like atom in a homogeneous magnetic field. The potential curves are eigenvalues corresponding to the angular oblate spheroidal functions that compose adiabatic basis which depends on the radial variable as a parameter. The matrix elements of radial coupling are integrals in angular variables of the following two types: product of angular functions and the first derivative of angular functions in parameter, and product of the first derivatives of angular functions in parameter, respectively. The program calculates also the angular part of the dipole transition matrix elements (in the length form) expressed as integrals in angular variables involving product of a dipole operator and angular functions. Moreover, the program calculates asymptotic regular and irregular matrix solutions of the coupled adiabatic radial equations at the end of interval in radial variable needed for solving a multi-channel scattering problem by the generalized **R**-matrix method. Potential curves and radial matrix elements computed by the POTHMF program can be used for solving the bound state and multi-channel scattering problems. As a test desk, the program is applied to the calculation of the energy values, a short-range reaction matrix and corresponding wave functions with the help of the KANTBP program. Benchmark calculations for the known photoionization cross-sections are presented.

Program summary

Program title: POTHMF
Catalogue identifier: AEAA_v1_0
Program summary URL: http://cpc.cs.qub.ac.uk/summaries/AEAA_v1_0.html
Program obtainable from: CPC Program Library, Queen's University, Belfast, N. Ireland
Licensing provisions: Standard CPC licence, http://cpc.cs.qub.ac.uk/licence/licence.html
No. of lines in distributed program, including test data, etc.: 8123
No. of bytes in distributed program, including test data, etc.: 131 396
Distribution format: tar.gz
Programming language: FORTRAN 77
Computer: Intel Xeon EM64T, Alpha 21264A, AMD Athlon MP, Pentium IV Xeon, Opteron 248, Intel Pentium IV
Operating system: OC Linux, Unix AIX 5.3, SunOS 5.8, Solaris, Windows XP

☆ This paper and its associated computer program are available via the Computer Physics Communications homepage on ScienceDirect (http://www.sciencedirect.com/science/journal/00104655).

* Corresponding author.
E-mail address: chuka@jinr.ru (O. Chuluunbaatar).

0010-4655/$ – see front matter
doi:10.1016/j.cpc.2007.09.005

RAM: Depends on

1. the number of radial differential equations;
2. the number and order of finite elements;
3. the number of radial points.

Test run requires 4 MB
Classification: 2.5
External routines: POTHMF uses some Lapack routines, copies of which are included in the distribution (see README file for details).
Nature of problem: In the multi-channel adiabatic approach the Schrödinger equation for a hydrogen-like atom in a homogeneous magnetic field of strength γ ($\gamma = B/B_0$, $B_0 \cong 2.35 \times 10^5$ T is a dimensionless parameter which determines the field strength B) is reduced by separating the radial coordinate, r, from the angular variables, (θ, φ), and using a basis of the angular oblate spheroidal functions [3] to a system of second-order ordinary differential equations which contain first-derivative coupling terms [4]. The purpose of this program is to calculate potential curves and matrix elements of radial coupling needed for calculating the low-lying bound and scattering states of hydrogen-like atoms in a homogeneous magnetic field of strength $0 < \gamma \leqslant 1000$ within the adiabatic approach [5]. The program evaluates also asymptotic regular and irregular matrix radial solutions of the multi-channel scattering problem needed to extract from the **R**-matrix a required symmetric shortrange open-channel reaction matrix **K** [6] independent from matching point [7]. In addition, the program computes the dipole transition matrix elements in the length form between the basis functions that are needed for calculating the dipole transitions between the low-lying bound and scattering states and photoionization cross sections [8].
Solution method: The angular oblate spheroidal eigenvalue problem depending on the radial variable is solved using a series expansion in the Legendre polynomials [3]. The resulting tridiagonal symmetric algebraic eigenvalue problem for the evaluation of selected eigenvalues, i.e. the potential curves, is solved by the $\mathbf{LDL}^{\mathrm{T}}$ factorization using the DSTEVR program [2]. Derivatives of the eigenfunctions with respect to the radial variable which are contained in matrix elements of the coupled radial equations are obtained by solving the inhomogeneous algebraic equations. The corresponding algebraic problem is solved by using the $\mathbf{LDL}^{\mathrm{T}}$ factorization with the help of the DPTTRS program [2]. Asymptotics of the matrix elements at large values of radial variable are computed using a series expansion in the associated Laguerre polynomials [9]. The corresponding matching points between the numeric and asymptotic solutions are found automatically. These asymptotics are used for the evaluation of the asymptotic regular and irregular matrix radial solutions of the multi-channel scattering problem [7]. As a test desk, the program is applied to the calculation of the energy values of the ground and excited bound states and reaction matrix of multi-channel scattering problem for a hydrogen atom in a homogeneous magnetic field using the KANTBP program [10].
Restrictions: The computer memory requirements depend on:

1. the number of radial differential equations;
2. the number and order of finite elements;
3. the total number of radial points.

Restrictions due to dimension sizes can be changed by resetting a small number of PARAMETER statements before recompiling (see Introduction and listing for details).
Running time: The running time depends critically upon:

1. the number of radial differential equations;
2. the number and order of finite elements;
3. the total number of radial points on interval $[r_{\min}, r_{\max}]$.

The test run which accompanies this paper took 7 s required for calculating of potential curves, radial matrix elements, and dipole transition matrix elements on a finite-element grid on interval $[r_{\min} = 0, r_{\max} = 100]$ used for solving discrete and continuous spectrum problems and obtaining asymptotic regular and irregular matrix radial solutions at $r_{\max} = 100$ for continuous spectrum problem on the Intel Pentium IV 2.4 GHz. The number of radial differential equations was equal to 6. The accompanying test run using the KANTBP program took 2 s for solving discrete and continuous spectrum problems using the above calculated potential curves, matrix elements and asymptotic regular and irregular matrix radial solutions. Note, that in the accompanied benchmark calculations of the photoionization cross-sections from the bound states of a hydrogen atom in a homogeneous magnetic field to continuum we have used interval $[r_{\min} = 0, r_{\max} = 1000]$ for continuous spectrum problem. The total number of radial differential equations was varied from 10 to 18.
References:

[1] W.H. Press, S.A. Teukolsky, W.T. Vetterling, B.P. Flannery, Numerical Recipes: The Art of Scientific Computing, Cambridge University Press, Cambridge, 1986.
[2] http://www.netlib.org/lapack/.
[3] M. Abramovits, I.A. Stegun, Handbook of Mathematical Functions, Dover, New York, 1965.
[4] U. Fano, Colloq. Int. C.N.R.S. 273 (1977) 127;
A.F. Starace, G.L. Webster, Phys. Rev. A 19 (1979) 1629–1640;
C.V. Clark, K.T. Lu, A.F. Starace, in: H.G. Beyer, H. Kleinpoppen (Eds.), Progress in Atomic Spectroscopy, Part C, Plenum, New York, 1984, pp. 247–320;
U. Fano, A.R.P. Rau, Atomic Collisions and Spectra, Academic Press, Florida, 1986.
[5] M.G. Dimova, M.S. Kaschiev, S.I. Vinitsky, J. Phys. B 38 (2005) 2337–2352;
O. Chuluunbaatar, A.A. Gusev, V.L. Derbov, M.S. Kaschiev, V.V. Serov, T.V. Tupikova, S.I. Vinitsky, Proc. SPIE 6537 (2007) 653706-1–18.
[6] M.J. Seaton, Rep. Prog. Phys. 46 (1983) 167–257.

[7] M. Gailitis, J. Phys. B 9 (1976) 843–854;
J. Macek, Phys. Rev. A 30 (1984) 1277–1278;
S.I. Vinitsky, V.P. Gerdt, A.A. Gusev, M.S. Kaschiev, V.A. Rostovtsev, V.N. Samoylov, T.V. Tupikova, O. Chuluunbaatar, Programming and Computer Software 33 (2007) 105–116.
[8] H. Friedrich, Theoretical Atomic Physics, Springer, New York, 1991.
[9] R.J. Damburg, R.Kh. Propin, J. Phys. B 1 (1968) 681–691;
J.D. Power, Phil. Trans. Roy. Soc. London A 274 (1973) 663–702.
[10] O. Chuluunbaatar, A.A. Gusev, A.G. Abrashkevich, A. Amaya-Tapia, M.S. Kaschiev, S.Y. Larsen, S.I. Vinitsky, Comput. Phys. Comm. 177 (2007) 649–675.

PACS: 02.60.Lj; 03.65.Nk; 31.15.Ja; 32.80.Fb; 33.55.Be

Keywords: Eigenvalue and multi-channel scattering problems; Kantorovich method; Finite element method; **R**-matrix calculation; Multi-channel adiabatic approximation; Ordinary differential equations; High-order accuracy approximation

1. Introduction

Nowadays the dynamics of transitional processes such as atomic scattering in the presence of an external confinement [1], channeling of light nuclei in a thin film with impurities [2], excitation, deexcitation [3], ionization and recombination of atoms and ions in magnetic traps is a subject of the experimental, theoretical and computational studies [4]. With the help of additional electric or laser pulse fields one can operate on transition rates and control the population of states in a quantum system for the above mentioned processes [5]. It is worth mentioning a recent study [6] of a new enhancement mechanism of a laser-stimulated recombination of antihydrogen in cold antiproton–positron plasma in a laboratory magnetic field B of order of few T via quasistationary states embedded in the continuum. To study optimal parameters of the laser and magnetic fields in complex cases such as when the Coulomb energy of an electron is comparable with energy of the magnetic field of strength γ in the axial gauge, one needs to develop really stable, inexpensive, highly efficient and accurate numerical methods and schemes required for calculations of the optical transitions between the bound and autoionization states of discrete and continuous spectra similar to the well known ones developed for the doubly-excited states of the Helium atom [7].

For an optimal account of correlations between the longitude and confined by the magnetic field transverse electron motion in cylindrical coordinates (z, ρ, φ) at fixed energy and azimuthal quantum number m, it is convenient to use transformation to the radial and angular variables, $r = \sqrt{z^2 + \rho^2}$, $\cos\theta = z/r$ [8]. Such transformation corresponds to the well-known change of coordinates (r_1, r_2) of the first and second electrons to hyperradius $r = \sqrt{r_1^2 + r_2^2}$ and hyperangle $\alpha = \arctan(r_1/r_2)$. This allows for an adequate account of radial correlations of electrons below the threshold for the Helium atom within the multi-channel hyperspherical adiabatic approach [9]. Main problems with the known approaches for solving the above problem are related to the necessity of constructing high accurate stable numerical schemes and solving ill-conditioned and/or large-scale algebraic problems that arise as a result of applying different approximations for the singular boundary problems in the two-dimensional region [10]. In order to provide a sufficiently high accuracy of calculations, most of popular methods require a large number of basis functions and often numerical integration over a large interval [11–18]. Bound state and continuum functions are usually calculated separately by different methods and the accuracy of these functions depends strongly on the accuracy of radial matrix elements used. Hence it is important to develop numerical methods for calculating potential matrix elements for the bound state and scattering problems that combine high accuracy with calculational scheme stability and high efficiency.

In this paper we present program POTHMF that realizes the multi-channel adiabatic approach in spherical coordinates for a hydrogen-like atom problem in a homogeneous magnetic field. An attractive feature of the adiabatic approach in spherical coordinates is that the electron wave function is accurately represented near the origin irrespective of the value of field strength. However, the problem here is how to match the spherically symmetric wave functions near the origin with the wave functions of the cylindrical symmetry which are more appropriate for areas located far enough from the origin [19]. In order to lower a dimension of the algebraic problem and improve its ill-condition property we use method suggested in [20]. It is based on (i) suitable analytic parameterizations of basis functions that satisfy boundary conditions and provide reasonable convergence and accuracy of expansion for a required solution, and (ii) constructing of proper asymptotic expansions of a solution in each of two independent variables to match analytic and numerical solutions after reduction of the singular boundary problem to a regular one (in a finite two-dimensional region).

From the mathematical point of view adiabatic approach is the Kantorovich method [21] which reduces a singular boundary problem for an elliptic partial differential equation in a two-dimensional region to a regular boundary problem for a system of the close-coupled ordinary second-order differential equations of a general type (with a skew-symmetric coefficient matrix of variable coefficients at the first derivatives) for calculating the bound and regular solutions for discrete and continuous spectra [10]. For a

given azimuthal quantum number m and z-parity, a solution depending on the radial variable r and angular variable $\eta = \cos\theta = z/r$ is expanded over the oblate angular spheroidal functions [22] in the angular variable that compose an orthogonal adiabatic basis parametrically depending on $p = \gamma r^2/2$. The most challenging part in realization of the Kantorovich method consists of the calculation of the coefficient matrices with the same given (machine precision) accuracy with which the eigenfunctions are computed.

In order to achieve this, the derivatives of angular functions with respect to parameter r are calculated as solutions of the nonhomogeneous boundary problem which is obtained by differentiating in parameter r the ordinary differential equation of the second order for the angular oblate spheroidal functions [22]. The corresponding algebraic eigenvalue problems (that arise as a result of the conventional representation of a solution at fixed magnetic quantum number m and z-parity by its expansion over normalized generalized Legendre polynomials [22]) are solved with the given accuracy at finite values of r by a stable symbolic–numerical algorithm [23]. Stability and economy of the numerical scheme is achieved due to the fact that for a small value of parameter r the angular functions become Legendre's polynomials while for a large value of r in the vicinities $\eta = \pm 1$ the angular functions become the associated Laguerre's functions in variables $y = 2(\gamma r^2/2)(1 \mp \eta)$, symmetrized in accordance to the z-parity property of angular oblate spheroidal functions for all values of parameter r [24]. The latter means that the sum and difference of these functions correspond to the z-even and z-odd solutions if one replaces η by $-\eta$. Therefore, for large r one could build asymptotic expansions in the inverse powers of r needed for calculation with a given accuracy of the required set of basis functions for all values of parameter r [23]. As a consequence, at large values of the radial variable r the potential curves, radial matrix elements and dipole transition matrix elements are calculated using asymptotic formulae and matching points $r_{\text{match}} < r_{\max}$ that are found automatically from the interval of integration $0 \leqslant r \leqslant r_{\max}$. It allows us to build a more economic algorithm for solving partial algebraic eigenvalue problem depending on parameter r with automatical choice of Wilkinson's shift [25].

Essential economy of computer resources for numerical solution of a boundary problem for a system of the radial second-order differential equations of general type (with matrix variable coefficients at the first derivative) is achieved by reducing the interval of integration $0 \leqslant r \leqslant r_{\max}$. In the present work, in order to do that we construct at large r ($r \geqslant r_{\max}$) an asymptotic expansion of fundamental solutions of a system of radial equations. A linear combination of Coulomb regular and irregular functions and their first derivatives is used here as a basis set. A choice of appropriate value of matching point $r = r_{\max}$ of the numerical regular solution for the radial problem on interval $0 \leqslant r \leqslant r_{\max}$ with the constructed asymptotic expansions is controlled by satisfying (with the optimal computer-dependent precision) of the conservation condition for the Wronskian with a long derivative. In the present work the KANTBP program [26] is used to calculate short-range reaction matrix $\mathbf{K}$ in open channels. The same matrix can be used for construction of solution of the auxiliary spectral problem in closed channels by applying the multi-channel quantum-defect theory (MQDT) [12,27], including additional (with respect to direct KANTBP calculations) eigenfunctions, eigenvalues and widths of closed channels.

The POTHMF program calculates potential curves and matrix elements of the coupled adiabatic radial equations for a hydrogen-like atom in a homogeneous magnetic field. It also computes the angular part of the dipole transition matrix elements (in the length form) between the angular functions and the asymptotic regular and irregular matrix solutions of a multi-channel scattering problem. Potential curves and radial matrix elements computed by the POTHMF program are used for solving the bound state and multi-channel scattering problems with the help of the KANTBP program [26]. As a test problem, the program is applied to the calculation of the energy values, short-range reaction matrix $\mathbf{K}$ and corresponding wave functions for a hydrogen-like atom in a homogeneous magnetic field. Benchmark calculations for the known photoionization cross-sections from the bound states ($1s_0$, $2p_{-1}$ and $3s_0$) of a hydrogen atom in a homogeneous magnetic field [12,15–17] are presented.

Efficiency of the elaborated program is demonstrated here by calculating photoionization cross-sections from the ground and low-lying excited states for a hydrogen atom to continuous state with $m = 0$. Note, that examples of application the proposed approach for calculation the low-lying excited states of a hydrogen atom in a homogeneous magnetic field $0 < \gamma \leqslant 1000$ together with analysis of convergence rate of the method using 10 radial equation are considered in [10]. Another application for calculation of continuous spectrum states and photoionization from $3d_0$ and $3s_0$ states to continuum at $\gamma = 2.595 \times 10^{-5}$ together with analysis of convergence rate of the method using 35 radial equation are given in [28]. The results of high-accurate calculation of a hydrogen atom photoionization cross-sections in a strong magnetic field using the POTHMF program are discussed in details in [29].

The paper is organized as follows. In Section 2 we give a brief overview of the problem. A description of the POTHMF algorithms are in Section 3. A description of the POTHMF program is given in Section 4. The subroutine units are briefly described in Section 5. The test problem is discussed in Section 6. Benchmark calculations for the photoionization cross-sections are given in Section 7.

2. Statement of the problem

The Schrödinger equation for the hydrogen atom in an axially symmetric homogeneous magnetic field $\mathbf{B} = (0, 0, B)$ in spherical coordinates (r, θ, φ) can be written as the 2D-equation [8]

$$\left(-\frac{1}{r^2}\frac{\partial}{\partial r}r^2\frac{\partial}{\partial r} + \frac{A^{(0)}(r,\theta)}{r^2} - \frac{2Z}{r} - \epsilon\right)\Psi(r,\theta) = 0 \tag{1}$$

in the region Ω: $0 < r < \infty$ and $0 < \theta < \pi$. The operator $A^{(0)}(r,\theta)$ is given by

$$A^{(0)}(r,\theta) = -\frac{1}{\sin\theta}\frac{\partial}{\partial\theta}\sin\theta\frac{\partial}{\partial\theta} + \frac{m^2}{\sin^2\theta} + \gamma m r^2 + \frac{1}{4}\gamma^2 r^4 \sin^2\theta, \tag{2}$$

where $m = 0, \pm 1, \ldots$ is the magnetic quantum number, $\gamma = B/B_0$, $B_0 \cong 2.35 \times 10^5$ T is a dimensionless parameter which determines the field strength B, and the atomic units (a.u.) $\hbar = m_e = e = 1$ are used under the assumption of infinite mass of the nucleus with a charge Z. In these expressions, $\epsilon = 2E$ is the doubled energy (in Rydbergs, 1 Ry $= (1/2)$ a.u.) of the bound state $|m\sigma\rangle$ at fixed values of m and z-parity; $\sigma = \pm 1$; and $\Psi \equiv \Psi_{m\sigma}(r,\theta) = (\Psi_m(r,\theta) + \sigma\Psi_m(r,\pi-\theta))/\sqrt{2}$ is the corresponding wave function. Here the sign of z-parity $\sigma = (-1)^{N_\theta}$ is defined by the number (even or odd) of nodes $N_\theta \equiv N_\eta$ in solution Ψ with respect to the angular variable θ in the interval $0 < \theta < \pi$. We will use also the scaled variable $\hat{r} = r\sqrt{\gamma}$, the effective charge $\hat{Z} = Z/\sqrt{\gamma}$ and the scaled energy $\hat{\epsilon} = \epsilon/\gamma$. It means that one can use unit cyclotron frequency and renormalize the initial charge Z by factor $\sqrt{1/\gamma}$ and initial energy ϵ by factor $1/\gamma$ only. The wave function satisfies the following boundary conditions in each $\mathbf{H}_{m\sigma}$ subspace of the full Hilbert space:

$$\lim_{\theta\to 0,\pi} \sin\theta\frac{\partial\Psi}{\partial\theta}(r,\theta) = 0, \quad \text{if } m = 0, \quad \text{and} \quad \Psi(r,0) = \Psi(r,\pi) = 0, \quad \text{if } m \neq 0, \tag{3}$$

$$\lim_{r\to 0} r^2\frac{\partial\Psi}{\partial r}(r,\theta) = 0. \tag{4}$$

The discrete spectrum wave function satisfies the asymptotic boundary condition approximated at large $r = r_{\max}$ by a boundary condition of the first type

$$\lim_{r\to\infty} r^2\Psi(r,\theta) = 0 \quad \to \quad \Psi(r_{\max},\theta) = 0. \tag{5}$$

Here the energy $\epsilon \equiv \epsilon(r_{\max})$ plays the role of eigenvalues of the boundary problem (1)–(5) on a finite interval $0 \leqslant r \leqslant r_{\max}$ with additional normalization condition

$$\int_0^{r_{\max}}\int_0^{\pi} r^2 \sin\theta \left|\Psi(r,\theta)\right|^2 dr\, d\theta = 1. \tag{6}$$

In the Fano–Lee $\mathbf{R}$-matrix theory [30,31] the continuum wave function $\Psi(r,\theta)$ satisfies the boundary condition of the third type at fixed values of energy ϵ and radial variable $r = r_{\max}$

$$\frac{\partial\Psi(r,\theta)}{\partial r} - \mu\Psi(r,\theta) = 0. \tag{7}$$

Here the parameters $\mu \equiv \mu(r_{\max},\epsilon)$, determined by the variational principle, play the role of eigenvalues of the logarithmic normal derivative matrix of the solution of the boundary problem (1)–(4), (7).

2.1. The KM reduction to a set of the radial differential equations

In the close coupling approximation, known in mathematics as the KM [21] the partial wave function $\Psi_i(r,\theta)$ is expanded over the one-parametric basis functions $\{\Phi_j^{m\sigma}(\theta;r)\}_{j=1}^N$

$$\Psi_i(r,\theta) = \sum_{j=1}^{N} \Phi_j^{m\sigma}(\theta;r)\chi_j^{(i)}(r). \tag{8}$$

In Eq. (8), the vector-function $\boldsymbol{\chi}^{(i)}(r) = (\chi_1^{(i)}(r),\ldots,\chi_N^{(i)}(r))^{\mathrm{T}}$ is unknown, and the surface functions $\boldsymbol{\Phi}^{m\sigma}(\theta;r) = (\Phi_1^{m\sigma}(\theta;r),\ldots,\Phi_N^{m\sigma}(\theta;r))^{\mathrm{T}}$ form an orthonormal basis with respect to the angular variable θ for each value of radius r which is treated here as a parameter. In the Kantorovich approach [21], the functions $\Phi_j(\theta;r) \equiv \Phi_j^{m\sigma}(\theta;r)$ are determined as solutions of the following parametric eigenvalue problem:

$$A^{(0)}(r,\theta)\Phi_j(\theta;r) = \varepsilon_j(r)\Phi_j(\theta;r). \tag{9}$$

The eigenfunctions of this problem satisfy the same boundary conditions in angular variable θ for $\Psi_i(r,\theta)$ and are normalized as follows

$$\left\langle\Phi_i(\theta;r)\middle|\Phi_j(\theta;r)\right\rangle_\theta = \int_0^{\pi} \sin\theta\,\Phi_i(\theta;r)\Phi_j(\theta;r)\,d\theta = \delta_{ij}, \tag{10}$$

where δ_{ij} is the Kronecker symbol.

After minimizing the Rayleigh–Ritz variational functional (see [32]) and using the expansion (8), Eq. (1) is reduced to a finite set of N ordinary second-order differential equations for the $\boldsymbol{\chi}(r) \equiv \boldsymbol{\chi}^{(i)}(r)$

$$\left(-\frac{1}{r^2}\mathbf{I}\frac{d}{dr}r^2\frac{d}{dr} + \mathbf{V}(r) + \mathbf{Q}(r)\frac{d}{dr} + \frac{1}{r^2}\frac{dr^2\mathbf{Q}(r)}{dr} - 2E\mathbf{I}\right)\boldsymbol{\chi}(r) = 0. \tag{11}$$

Here $\mathbf{I}$, $\mathbf{V}(r)$ and $\mathbf{Q}(r)$ are $N \times N$ matrices whose elements are given by the relation

$$\begin{aligned}
&V_{ij}(r) = H_{ij}(r) + \left(\frac{\varepsilon_i(r) + \varepsilon_j(r)}{2r^2} - \frac{2Z}{r}\right)\delta_{ij}, \qquad I_{ij} = \delta_{ij},\\
&H_{ij}(r) = H_{ji}(r) = \left\langle \frac{\partial\Phi_i(\theta;r)}{\partial r}\middle|\frac{\partial\Phi_j(\theta;r)}{\partial r}\right\rangle_\theta,\\
&Q_{ij}(r) = -Q_{ji}(r) = -\left\langle \Phi_i(\theta;r)\middle|\frac{\partial\Phi_j(\theta;r)}{\partial r}\right\rangle_\theta.
\end{aligned} \tag{12}$$

The wave function $\boldsymbol{\chi}(r)$ satisfies the following boundary conditions at $r \to 0$

$$\lim_{r\to 0} r^2\left(\mathbf{I}\frac{d}{dr} - \mathbf{Q}(r)\right)\boldsymbol{\chi}(r) = 0, \tag{13}$$

and at $r = r_{\max}$

$$\boldsymbol{\chi}(r) = 0, \quad \text{for the discrete spectrum,} \tag{14}$$

$$\left(\mathbf{I}\frac{d}{dr} - \mathbf{Q}(r)\right)\boldsymbol{\chi}(r) = \mu(r)\boldsymbol{\chi}(r), \quad \text{for the continuous spectrum.} \tag{15}$$

3. Description of the POTHMF algorithms

3.1. Calculation of the angular oblate spheroidal functions

Note, that the solutions of the problem (9), (2) with the shifted eigenvalues $\lambda_j(p) = \varepsilon_j(r) - \gamma m r^2$ correspond to the solutions of the eigenvalue problem for the angular oblate spheroidal functions [22] with respect to a variable $\eta = \cos\theta$:

$$-\frac{\partial}{\partial\eta}(1-\eta^2)\frac{\partial\Phi_j(\eta;p)}{\partial\eta} + \left(\frac{m^2}{1-\eta^2} + p^2(1-\eta^2)\right)\Phi_j(\eta;p) = \lambda_j(p)\Phi_j(\eta;p), \tag{16}$$

where $p = \hat{r}^2/2 = \gamma r^2/2$, and eigenfunctions $\Phi_j(\eta;p)$ satisfy the orthogonality conditions (10). We obtain eigenfunctions $\Phi_j(\eta;r) \equiv \Phi_j(\eta;p)$ in the form of a series expansion at fixed values $\sigma = \pm 1$ and m,

$$\Phi_j(\eta;r) = \sum_{s=(1-\sigma)/2}^{s_{\max}} c_{sj}^{m\sigma}(r) P_{|m|+s}^{|m|}(\eta). \tag{17}$$

Here s is the even (odd) integer at $\sigma = (-1)^s = \pm 1$ up to $s_{\max} = 2(N_{\max} - 1) + (1-\sigma)/2$, where $N_{\max}$ is number of even or odd terms of expansion, $P_{|m|+s}^{|m|}(\eta)$ are the normalized associated Legendre polynomials [22]. The coefficients $c_{sj}^{m\sigma}(r)$ satisfy the relation

$$\sum_{s=(1-\sigma)/2}^{s_{\max}} c_{sj}^{m\sigma}(r) c_{sj'}^{m\sigma}(r) = \delta_{jj'}. \tag{18}$$

The eigenvalue problem for eigenvectors $\mathbf{c}_j = \{c_{sj}^{m\sigma}(r)\}_{(1-\sigma)/2}^{s_{\max}}$, and eigenvalues $\lambda_j \equiv \lambda_j(p)$ take the form

$$\mathbf{A}^{(0)}\mathbf{c}_j = \lambda_j \mathbf{c}_j, \tag{19}$$

$$\mathbf{c}_j^{\mathrm{T}}\mathbf{c}_j = \mathbf{I}, \tag{20}$$

where matrix $\mathbf{A}^{(0)} \equiv \mathbf{A}^{(0)}(p)$ is the symmetric tridiagonal $N_{\max} \times N_{\max}$ matrix:

$$\begin{aligned}
&A_{ss-2}^{(0)} = A_{s-2s}^{(0)} = \frac{-p^2}{(2s+2|m|-1)}\sqrt{\frac{(s-1)s(s+2|m|-1)(s+2|m|)}{(2s+2|m|-3)(2s+2|m|+1)}},\\
&A_{ss}^{(0)} = \big(s+|m|\big)\big(s+|m|+1\big) + 2p^2\frac{(s^2+s+2s|m|+2m^2+|m|-1)}{(2s+2|m|-1)(2s+2|m|+3)}.
\end{aligned} \tag{21}$$

The expansion (17) was used which provides stability of numerical calculation with the double precision arithmetic (the relative machine precision is $eps = 2^{-52} \approx 2 \cdot 10^{-16}$) with the help of the subroutine DSTEVR from the LAPACK Fortran Library [33]. The orthogonality relations (18) were fulfilled with an accuracy of the order of eps.

3.2. Evaluation of parametric derivative of the angular functions and matrix elements

Radial matrix elements in notations of coefficient $\mathbf{c}_j$ of decomposition (17) have the following form

$$Q_{ij}(r) = -\mathbf{c}_i^{\mathrm{T}}\mathbf{c}_j^{(1)}, \qquad H_{ij}(r) = \left(\mathbf{c}_i^{(1)}\right)^{\mathrm{T}}\mathbf{c}_j^{(1)}, \tag{22}$$

where $\mathbf{c}_j^{(1)} = d\mathbf{c}_j/dr$.

Step 1. As follows from (19), we should solve the following linear set of algebraic equations

$$\mathbf{A}^{(1)}\mathbf{c}^{(0)} - \mathbf{c}^{(0)}\lambda^{(1)} = -(\mathbf{A}^{(0)}\mathbf{c}^{(1)} - \mathbf{c}^{(1)}\lambda^{(0)}), \qquad \mathbf{A}^{(1)} \equiv \frac{d\mathbf{A}^{(0)}}{dr}, \tag{23}$$

where $\mathbf{c}^{(0)} \equiv \mathbf{c}_j$, $\lambda^{(0)} \equiv \lambda_j$, $\mathbf{c}^{(1)} \equiv \mathbf{c}_j^{(1)}$ and $\lambda^{(1)} \equiv d\lambda_j/dr$.

Step 2. Taking into account that $\lambda^{(0)}$ is an eigenvalue of the operator defined in (19), the problem (23) has a solution *if and only if the right-hand side term is orthogonal to the eigenfunction* $\mathbf{c}^{(0)}$. Multiplying (23) by $(\mathbf{c}^{(0)})^{\mathrm{T}}$ and using the normalization condition (20), we obtain the expression for $\lambda^{(1)}$

$$\lambda^{(1)} = (\mathbf{c}^{(0)})^{\mathrm{T}}\mathbf{A}^{(1)}\mathbf{c}^{(0)} \tag{24}$$

and the set of the inhomogeneous algebraic equations for unknown vector $\mathbf{c}^{(1)}$

$$\mathbf{L}\mathbf{c}^{(1)} \equiv \mathbf{A}^{(0)}\mathbf{c}^{(1)} - \mathbf{c}^{(1)}\lambda^{(0)} = \mathbf{b}^{(1)}, \qquad \mathbf{b}^{(1)} = -\mathbf{A}^{(1)}\mathbf{c}^{(0)} + \mathbf{c}^{(0)}\lambda^{(1)}. \tag{25}$$

Now the problem (25) has a solution, but it is not unique. From the normalization condition (20) we obtain the required additional equality

$$(\mathbf{c}^{(1)})^{\mathrm{T}}\mathbf{c}^{(0)} = 0, \tag{26}$$

providing the uniqueness of the solution (25). Since $\lambda^{(0)}$ is an eigenvalue of (19), the matrix $\mathbf{L}$ in (25) is degenerate.

Note, if matrix $\mathbf{A}^{(0)}$ is diagonal, then the solution of system (25)–(26) can be evaluated analytically. The algorithm for numerical solution of (25) in a case of nondiagonal matrix $\mathbf{A}^{(0)}$ can be written in three steps as follows:

Step 3. Calculate solutions $\mathbf{v}^{(1)}$ and $\mathbf{w}$ of the auxiliary inhomogeneous set algebraic equations

$$\bar{\mathbf{L}}\mathbf{v}^{(1)} = \bar{\mathbf{b}}^{(1)}, \qquad \bar{\mathbf{L}}\mathbf{w} = \mathbf{d}, \tag{27}$$

with nondegenerate matrix $\bar{\mathbf{L}}$ and right-hand sides $\bar{\mathbf{b}}^{(1)}$ and $\mathbf{d}$

$$\bar{L}_{ss'} = \begin{cases} L_{ss'}, & (s-S)(s'-S) \neq 0, \\ \delta_{ss'}, & (s-S)(s'-S) = 0, \end{cases} \tag{28}$$

$$\bar{b}_s^{(1)} = \begin{cases} b_s^{(1)}, & s \neq S, \\ 0, & s = S, \end{cases} \qquad d_s = \begin{cases} L_{sS}, & s \neq S, \\ 0, & s = S, \end{cases} \tag{29}$$

where S is the number of the greatest absolute value element of vector $\mathbf{c}^{(0)}$.

Step 4. Evaluate coefficient $\gamma^{(1)}$

$$\gamma^{(1)} = -\frac{\gamma_1^{(1)}}{(c_S^{(0)} - \gamma_2)}, \qquad \gamma_1^{(1)} = (\mathbf{v}^{(1)})^{\mathrm{T}}\mathbf{c}^{(0)}, \qquad \gamma_2 = \mathbf{w}^{\mathrm{T}}\mathbf{c}^{(0)}. \tag{30}$$

Step 5. Evaluate vector $\mathbf{c}^{(1)}$

$$c_s^{(1)} = \begin{cases} v_s^{(1)} - \gamma^{(1)}w_s, & s \neq S, \\ \gamma^{(1)}, & s = S. \end{cases} \tag{31}$$

The above algorithm for calculation of matrix elements was implemented in the MAPLE and FORTRAN (general algorithms for evaluation of high-order derivatives of the eigenvalues, eigenvectors and corresponding matrix elements are discussed in [23]). The algorithm provides stability of numerical calculation with double precision arithmetic (the relative machine precision is $eps = 2^{-52} \approx 2 \cdot 10^{-16}$) with help of the subroutine DPTTRS from the LAPACK Fortran Library [33].

3.3. Asymptotics of oblate angular spheroidal functions and matrix elements

At small r, asymptotic values of matrix elements $\varepsilon_j(r)$, $H_{jj'}(r)$ and $Q_{jj'}(r)$ characterized by $l = |m| + s = 2j - 2 + |m|$ for even states ($\sigma = (-1)^{l-|m|} = +1$) and $l = |m| + s = 2j - 1 + |m|$ for odd states ($\sigma = (-1)^{l-|m|} = -1$) are the series expansion by the power of r at some finite values l_l, l_r [23]

$$\varepsilon_j(r) = \bar{\varepsilon}_j^{(0)} + \bar{\varepsilon}_j^{(2)} r^2 + \sum_{k=1}^{k_{\max}} r^{4k} \bar{\varepsilon}_j^{(4k)}, \qquad H_{jj'}(r) = \sum_{k=2}^{k_{\max}} r^{4k-2} \bar{H}_{jj'}^{(4k-2)},$$
$$Q_{jj'}(r) = \sum_{k=1}^{k_{\max}} r^{4k-1} \bar{Q}_{jj'}^{(4k-1)}. \tag{32}$$

The above matrix elements have been calculated analytically using the algorithm implemented in MAPLE up to $k_{\max} = 4$. Below we present the first few coefficients of matrix elements:

$$\bar{\varepsilon}_j^{(0)} = \lambda_s^{m\sigma}(0) = l(l+1), \qquad \bar{\varepsilon}_j^{(2)} = \gamma m, \qquad \bar{\varepsilon}_j^{(4)} = \frac{\gamma^2}{2} \frac{l^2 + l - 1 + m^2}{(2l-1)(2l+3)},$$
$$\bar{Q}_{jj+2}^{(3)} = \frac{\gamma^2}{2} \frac{\sqrt{(l+1)^2 - m^2}\sqrt{(l+2)^2 - m^2}}{\sqrt{2l+1}(2l+3)^2\sqrt{2l+5}},$$
$$\begin{aligned}\bar{H}_{jj}^{(6)} = \frac{\gamma^4}{2}\big(&(16l^4 + 32l^3 + 248l^2 + 232l + 201)m^4 \\ &+ (-10l^2 - 224l^4 - 96l^5 + 118l - 288l^3 - 32l^6 - 195)m^2 \\ &+ 16l^8 + 64l^7 + 46l + 40l^6 - 127l^4 - 104l^5 + 71l^2 - 6l^3 - 6\big) \\ &/\big((2l-3)(2l-1)^4(2l+3)^4(2l+5)\big),\end{aligned}$$
$$\bar{H}_{jj+4}^{(6)} = \frac{-\gamma^4\sqrt{(l+1)^2 - m^2}\sqrt{(l+2)^2 - m^2}\sqrt{(l+3)^2 - m^2}\sqrt{(l+4)^2 - m^2}}{4\sqrt{2l+1}(2l+3)^2(2l+5)(2l+7)^2\sqrt{2l+9}}. \tag{33}$$

This asymptotic behavior of effective potentials allows us to use the above boundary conditions (13) at $r \to 0$ to find regular and bounded solutions. Note, that these asymptotic expansions have a finite radius of convergence because the parameter r has branch points in the complex plane [34–36].

Matrix elements at large r can be evaluated as series expansions by the inverse power of p up to the order of $k_{\max}$ without taking into account the exponential small terms. For this we use the eigenfunctions $\boldsymbol{\Phi}^{m\leftarrow}(\eta; r)$ and $\boldsymbol{\Phi}^{m\rightarrow}(\eta; r)$ localized at large r in vicinity of $\eta = \pm 1$

$$\boldsymbol{\Phi}^{m\sigma=\pm 1}(\eta; r) = \frac{\boldsymbol{\Phi}^{m\rightarrow}(\eta; r) \pm \boldsymbol{\Phi}^{m\leftarrow}(\eta; r)}{\sqrt{2}}. \tag{34}$$

These functions have $N_\rho \equiv n = 0, 1, 2, \ldots$, nodes in the subintervals $0 < \eta < 1$ and $-1 < \eta < 0$, respectively, i.e. $N_\rho = N_\eta/2$ for the even z-parity states, $\sigma = +1$, and $N_\rho = (N_\eta - 1)/2$ for the odd z-parity states, $\sigma = -1$, where N_η is number of nodes $\boldsymbol{\Phi}^{m\sigma}(\eta; r)$ in the interval $-1 < \eta < 1$ with parity $\sigma = (-1)^{N_\eta}$. Note, that $\boldsymbol{\Phi}^{m\leftarrow}(\eta; r) = \boldsymbol{\Phi}^{m\rightarrow}(-\eta; r)$ and $\boldsymbol{\Phi}^{m\leftarrow}(\eta < 0; r) = \boldsymbol{\Phi}^{m\rightarrow}(\eta > 0; r) = \mathrm{O}(\exp(-p(1 + |\eta|)))$ at $r \to \infty$ and $|\eta| \sim 1$ and will be used in a construction of the scattering wave functions defined in (73).

Matrix elements are represented as the series expansion by the inverse power of r without the exponential terms in accordance with [23]

$$r^{-2}\varepsilon_j(r) = \varepsilon_j^{(0)} + \sum_{k=1}^{k_{\max}} r^{-2k} \varepsilon_j^{(2k)}, \qquad H_{jj'}(r) = \sum_{k=1}^{k_{\max}} r^{-2k} H_{jj'}^{(2k)},$$
$$Q_{jj'}(r) = \sum_{k=1}^{k_{\max}} r^{1-2k} Q_{jj'}^{(2k-1)}. \tag{35}$$

Here $\epsilon_{mj}^{th}(\gamma) = \varepsilon_j^{(0)}$ is an energy of the thresholds (in Ry) that corresponds to the double energy of the Landau thresholds (in a.u.).

In the present work, the calculation was performed by the algorithm implemented in MAPLE up to the $k_{\max} = 8$. Below we display the first several coefficients of potential curves $\varepsilon_j(r)$ at fixed m

$$\varepsilon_j^{(0)} = \gamma\big(2n + m + |m| + 1\big),$$
$$\varepsilon_j^{(2)} = -2n^2 - 2n|m| - 2n - |m| - 1, \tag{36}$$

and matrix elements $Q_{jj'}(r)$, $H_{jj'}(r)$

$$
\begin{aligned}
Q^{(1)}_{jj'} &= (n_r - n_l)\sqrt{n+1}\sqrt{n+|m|+1}\delta_{|n_l-n_r|1},\\
Q^{(3)}_{jj'} &= (4\gamma)^{-1}(n_r - n_l)\sqrt{n+1}\sqrt{n+|m|+1}\\
&\quad\times\left(2(2n+|m|+2)\delta_{|n_l-n_r|1} + \sqrt{n+2}\sqrt{n+|m|+2}\,\delta_{|n_l-n_r|2}\right),\\
H^{(2)}_{jj'} &= \left(2n^2+2n+2|m|n+|m|+1\right)\delta_{|n_l-n_r|0}\\
&\quad-\sqrt{n+1}\sqrt{n+|m|+1}\sqrt{n+2}\sqrt{n+|m|+2}\delta_{|n_l-n_r|2}.
\end{aligned}
\tag{37}
$$

In these formulas asymptotic quantum number $n = \min(n_l, n_r)$ denote transversal quantum number that is connected with the unified numbers j and j' by the formulas $n_l = j - 1$ and $n_r = j' - 1$. Note, that $\varepsilon^{(2)}_j + H^{(2)}_{jj} = 0$, i.e. at large r the centrifugal terms are eliminated in Eq. (11). It means that the leading terms of radial solutions $\chi_{ji_o}(r)$ have the same asymptotics as the Coulomb functions with a zero angular momentum and the effective charge $\hat{Z}$ in terms of the scaled radial variable $\hat{r}$. The convergence of expansion (35) is shown in [23]. Note, that evaluating the exponential small corrections (for improving the convergence) can be done using additional series expansion of the solution in the region $D_2 = [0, 1-\eta_2]$, $\eta_2 < \eta_1$, $\eta_2 = \mathrm{o}(p^{-1/2-\varepsilon})$ in accordance with [37].

3.4. Longitudinal and transversal dipole matrix elements

The longitudinal dipole matrix elements $\mathbf{D}^{(m\sigma\sigma')}(r)$ with photon linearly polarized along z axis and transversal ones $\mathbf{P}^{(mm'\sigma)}(r)$ with photon circularly polarized in XOY plane are expressed as

$$
D^{(m\sigma\sigma')}_{jj'}(r) = \left\langle \Phi^{m\sigma}_j(\eta;r)\middle| r\eta \middle| \Phi^{m\sigma'=-\sigma}_{j'}(\eta;r)\right\rangle_\eta,
\tag{38}
$$

$$
P^{(mm'\sigma)}_{jj'}(r) = \left\langle \Phi^{m\sigma}_j(\eta;r)\middle| r\frac{\sqrt{1-\eta^2}}{\sqrt{2}} \middle| \Phi^{m'=m\pm1\sigma}_{j'}(\eta;r)\right\rangle_\eta.
\tag{39}
$$

Using expression (17) the above matrix elements can be written in the form

$$
\begin{aligned}
D^{(m\sigma\sigma')}_{jj'}(r) &= r\sum_{s=(1-\sigma)/2}^{s_{\max}}\sum_{s'=(1-\sigma')/2}^{s_{\max}} c^{m\sigma}_{sj}(r)c^{m\sigma'}_{s'j'}(r)\int_{-1}^{1}\eta P^{|m|}_{|m|+s}(\eta)P^{|m|}_{|m|+s'}(\eta)\,d\eta\\
&= \delta_{|\sigma+\sigma'|0} r\sum_{s=(1-\sigma)/2}^{s_{\max}}\sum_{s'=(1-\sigma')/2}^{s_{\max}} c^{m\sigma}_{sj}(r)c^{m\sigma'}_{s'j'}(r)\delta_{|s-s'|1}\frac{\sqrt{s_>}\sqrt{s_>+2|m|}}{\sqrt{4(s_>+|m|)^2-1}},
\end{aligned}
\tag{40}
$$

$$
\begin{aligned}
P^{(mm'\sigma)}_{jj'}(r) &= \frac{r}{\sqrt{2}}\sum_{s=(1-\sigma)/2}^{s_{\max}}\sum_{s'=(1-\sigma)/2}^{s_{\max}} c^{m\sigma}_{sj}(r)c^{m'\sigma}_{s'j'}(r)\int_{-1}^{1}\sqrt{1-\eta^2}P^{|m|}_{|m|+s}(\eta)P^{|m'|}_{|m'|+s'}(\eta)\,d\eta\\
&= \delta_{|m-m'|1}\frac{r}{\sqrt{2}}\sum_{s=(1-\sigma)/2}^{s_{\max}}\sum_{s'=(1-\sigma)/2}^{s_{\max}} c^{m\sigma}_{sj}(r)c^{m'\sigma}_{s'j'}(r)\\
&\quad\times\left[\delta_{ss'+2}\sqrt{\frac{s(s-1)}{(2s+2m_<-1)(2s+2m_<+1)}} - \delta_{ss'}\sqrt{\frac{(s+2m_<+1)(s+2m_<+2)}{(2s+2m_<+1)(2s+2m_<+3)}}\right],
\end{aligned}
\tag{41}
$$

where $s_> = \max(s, s')$ and $m_< = \min(|m|, |m'|)$.

3.5. Asymptotics of longitudinal and transversal dipole matrix elements

We find longitudinal and transversal dipole matrix elements as the series expansion by the inverse power of r without the exponential terms

$$
D^{(m\sigma\sigma')}_{jj'}(r) = r\sum_{k=0}^{k_{\max}} r^{-2k}D^{(2k)}_{jj'}, \qquad P^{(mm'\sigma)}_{jj'}(r) = -\sum_{k=0}^{k_{\max}} r^{-2k}P^{(2k)}_{jj'}.
\tag{42}
$$

In these formulas asymptotic quantum number n denotes transversal quantum number connected with the unified numbers j and j' by the formulas $n_l = j - 1$ and $n_r = j' - 1$.

The calculation was performed using the algorithm implemented in MAPLE up to $k_{\max} = 8$. Below we display the first few coefficients of the longitudinal dipole matrix $\mathbf{D}^{(m\sigma\sigma')}(r)$ at fixed m

$$
\begin{aligned}
D^{(0)}_{jj'} &= \delta_{|n_l - n_r|0}, \\
D^{(2)}_{jj'} &= \gamma^{-1}\big(-(2n + |m| + 1)\delta_{|n_l - n_r|0} + \sqrt{n}\sqrt{n + |m|}\delta_{|n_l - n_r|1}\big),
\end{aligned} \tag{43}
$$

and the transversal dipole matrix $\mathbf{P}^{(mm'\sigma)}(r)$ at fixed $|m'| = |m| + 1$

$$
\begin{aligned}
P^{(0)}_{jj'} &= \gamma^{-1/2}\big(\sqrt{n_l + |m| + 1}\delta_{n_l n_r} - \sqrt{n_l}\delta_{n_l n_r + 1}\big), \\
P^{(2)}_{jj'} &= 2^{-1}\gamma^{-3/2}\big(-\sqrt{n_l}\sqrt{n_l - 1}\sqrt{n_l + |m|}\delta_{n_l n_r + 2} \\
&\quad + \sqrt{n_l + 1}\sqrt{n_l + |m| + 1}\sqrt{n_l + |m| + 2}\delta_{n_l n_r - 1}\big),
\end{aligned} \tag{44}
$$

where $n = \min(n_l, n_r)$. Note, that the asymptotic longitudinal dipole matrix $\mathbf{D}^{(m\sigma\sigma')}(r)$ is symmetric for σ and σ', and the asymptotic transversal dipole matrix $\mathbf{P}^{(mm'\sigma)}(r)$ is nonsymmetric but satisfies the relation $P^{(mm'\sigma)}_{jj'}(r) = P^{(m'm\sigma)}_{j'j}(r)$.

3.6. *Finding optimal value of $s_{\max}$ and matching point r_{match} of numerical and asymptotic solutions*

At large s elements of matrix $\mathbf{A}^{(0)}$ (21) take form

$$
\begin{aligned}
A^{(0)}_{ss} &= \frac{(2s + 2|m| + 1)^2 - 1}{4} + \frac{p^2}{2} + \mathrm{O}(s^{-2}), \\
A^{(0)}_{ss+2} &= A^{(0)}_{ss-2} = -\frac{p^2}{4} + \mathrm{O}(s^{-2}).
\end{aligned} \tag{45}
$$

On intervals $s \in (s_b, s_e)$ at $s_b, s_e \gg 1$, we suppose that the elements of matrix $\mathbf{A}^{(0)}$ have slow dependence on s. Therefore, for a given value of λ solution of algebraic problem (19), (45) will be represented in the form

$$
c_s = x c_{s+2}, \quad c_{s-2} = x c_s. \tag{46}
$$

From (46), (19), (45) we have algebraic equation with respect to factor x

$$
x + \frac{1}{x} = d \equiv \frac{(2s + 2|m| + 1)^2 - 1 - 4\lambda + 2p^2}{p^2}. \tag{47}
$$

For $s > s_2$, where s_2 is determined from Eq. (47) at $d = 2$,

$$
s_2 = \frac{\sqrt{4\lambda + 1} - 2|m| - 1}{2}, \tag{48}
$$

Eq. (47) has two real solutions. One of them,

$$
x_s = \frac{(\sqrt{(s - s_2)(s + s_2 + 2|m| + 1)} + \sqrt{p^2 + (s - s_2)(s + s_2 + 2|m| + 1)})^2}{p^2}, \tag{49}
$$

is greater by absolute value then unity and the other, $1/x_s$, is smaller one. It means that the solution of (46) with decreased coefficients c_s at increased s exists. For $s < s_2$ we have two solutions with oscillating coefficients c_s. Then solution of Eq. (47), allows us to determine algorithm for evaluation $s_{\max}$:

$$
\prod_{s=s_2}^{s_{\max}-1} x_s < 1/eps, \qquad \prod_{s=s_2}^{s_{\max}} x_s > 1/eps, \tag{50}
$$

where $eps = 2^{-52} \approx 2 \cdot 10^{-16}$ is the relative machine precision.

We need an approximate value of the eigenvalue λ for the above calculation. If we use the fact all diagonal elements $A^{(0)}_{ss}$ of the tridiagonal matrix $\mathbf{A}^{(0)}$ and eigenvalues $\varepsilon_j(p)$ or $\lambda_j(p)$ increased by number j, then we can obtain the upper bound of the eigenvalue λ_N with the help of Wilkinson's shift [25]

$$
shift = G + A^{(0)}_{s_N s_N} + \sqrt{G^2 + (A^{(0)}_{s_N s_N - 2})^2}, \qquad G = \frac{A^{(0)}_{s_N - 2 s_N - 2} - A^{(0)}_{s_N s_N}}{2}, \tag{51}
$$

where $s_N = 2(N - 1) + (1 - \sigma)/2$. But $shift \gg \lambda_N$ at $p \gg 1$. It this case we use asymptotic expression of the eigenvalue (35) at $p \geqslant 2s_N$, since the asymptotic expression gives an upper bound of the eigenvalue.

The matching point $r_{\rm match}$ of the numerical and asymptotic solution is calculated as follows

$$r_{\rm match} = \max(r_\varepsilon, r_h, r_q),$$
$$r_\varepsilon = \sqrt[18]{\frac{|\varepsilon_N^{(18)}|}{eps}}, \qquad r_h = \sqrt[18]{\frac{|H_{NN}^{(18)}|}{eps}}, \qquad r_q = \sqrt[17]{\frac{|Q_{NN-1}^{(17)}|}{eps}}, \tag{52}$$

since $|\varepsilon_j^{(2k)}| < \gamma|\varepsilon_j^{(2k+2)}|$, $|Q_{jj'}^{(2k-1)}| < \gamma|Q_{jj'}^{(2k+1)}|$, $|H_{jj'}^{(2k)}| < \gamma|H_{jj'}^{(2k+2)}|$ and $|Q_{jj'}^{(17)}| \leqslant |Q_{NN-1}^{(17)}|$, $|H_{jj'}^{(18)}| \leqslant |H_{NN}^{(18)}|$.

The matching points $r_{\rm match} = r_d$ and $r_{\rm match} = r_p$ of the numerical and asymptotic solution are calculated follows

$$r_d = \sqrt[17]{\frac{|D_{NN}^{(18)}|}{eps}}, \qquad r_p = \sqrt[18]{\frac{\max(|P_{N-1N}^{(18)}|, |P_{NN-1}^{(18)}|)}{eps}}, \tag{53}$$

since $|D_{jj'}^{(2k)}| < \gamma|D_{jj'}^{(2k+2)}|$, $|P_{jj'}^{(2k)}| < \gamma|P_{jj'}^{(2k+2)}|$, $|D_{jj'}^{(18)}| \leqslant |D_{NN}^{(18)}|$, $|P_{jj'}^{(18)}| \leqslant \max(|P_{N-1N}^{(18)}|, |P_{NN-1}^{(18)}|)$.

3.7. Construction of regular and irregular matrix-solutions

Now let us consider the asymptotic solution following [38]

$$\chi_{ji_o}(r) = R(p_{i_o}, r)\phi_{ji_o}(r) + \frac{dR(p_{i_o}, r)}{dr}\psi_{ji_o}(r), \tag{54}$$

$$\phi_{ji_o}(r) = \sum_{k=0}^{k_{\max}} \phi_{ji_o}^{(k)} r^{-k}, \qquad \psi_{ji_o}(r) = \sum_{k=0}^{k_{\max}} \psi_{ji_o}^{(k)} r^{-k}, \tag{55}$$

where $R(p_{i_o}, r) = p_{i_o}^{-1/2} r^{-1}(\imath\, F_0(p_{i_o}, r) + G_0(p_{i_o}, r))/2$, $F_0(p_{i_o}, r)$ and $G_0(p_{i_o}, r)$ are the Coulomb regular and irregular functions, respectively [22]. These functions satisfy the condition

$$G_0(p_{i_o}, r)\frac{dF_0(p_{i_o}, r)}{dr} - \frac{dG_0(p_{i_o}, r)}{dr}F_0(p_{i_o}, r) = p_{i_o}. \tag{56}$$

After substituting the expansions (55) into Eq. (11) and equating the coefficients at the same powers of r we arrive at the set of recurrence relations with respect to the unknown coefficients $\phi_{ji_o}^{(k)}$ and $\psi_{ji_o}^{(k)}$:

$$\begin{aligned}
&\big(p_{i_o}^2 - 2E + \varepsilon_j^{(0)}\big)\phi_{ji_o}^{(k)} - 2p_{i_o}^2(k-1)\psi_{ji_o}^{(k-1)} - (k-2)(k-3)\phi_{ji_o}^{(k-2)} \\
&\quad - 2Z(2k-3)\psi_{ji_o}^{(k-2)} + \sum_{k'=1}^{k}\big(\varepsilon_j^{(k')} + H_{jj}^{(k')}\big)\phi_{ji_o}^{(k-k')} \\
&= \sum_{j'=1, j'\neq j}^{N}\sum_{k'=1}^{k}\Big[\big((2k-k'-3)Q_{jj'}^{(k'-1)} - H_{jj'}^{(k')}\big)\phi_{j'i_o}^{(k-k')} \\
&\quad + \big(2p_{i_o}^2 Q_{jj'}^{(k')} + 4ZQ_{jj'}^{(k'-1)}\big)\psi_{j'i_o}^{(k-k')}\Big],
\end{aligned} \tag{57}$$

$$\begin{aligned}
&\big(p_{i_o}^2 - 2E + \varepsilon_j^{(0)}\big)\psi_{ji_o}^{(k)} + 2(k-1)\phi_{ji_o}^{(k-1)} - k(k-1)\psi_{ji_o}^{(k-2)} + \sum_{k'=1}^{k}\big(\varepsilon_j^{(k')} + H_{jj}^{(k')}\big)\psi_{ji_o}^{(k-k')} \\
&= \sum_{j'=1, j'\neq j}^{N}\sum_{k'=1}^{k}\Big[\big((2k-k'+1)Q_{jj'}^{(k'-1)} - H_{jj'}^{(k')}\big)\psi_{j'i_o}^{(k-k')} - 2Q_{jj'}^{(k')}\phi_{j'i_o}^{(k-k')}\Big].
\end{aligned} \tag{58}$$

We get the leading terms of the eigenfunction, the eigenvalue $p_{i_o}^2$, i.e. the initial data for solving the above recurrence equations from (57) and (58), as shown in [23]

$$\phi_{j_0 i_o}^{(0)} = \delta_{j_0 i_o}, \qquad \psi_{j_0 i_o}^{(0)} = 0, \qquad p_{i_o}^2 = 2E - \varepsilon_{i_o}^{(0)}, \tag{59}$$

that correspond to the leading term of $\chi_{ji_o}(r)$ satisfying the asymptotic expansion at large r

$$\chi_{ji_o}(r) = \frac{\exp(\imath p_{i_o} r + \imath\zeta\ln(2p_{i_o}r) + \imath\delta_{i_o}^c)}{2r\sqrt{p_{i_o}}}\delta_{ji_o}, \quad \zeta = \frac{Z}{p_{i_o}}, \tag{60}$$

where ζ is the Sommerfeld parameter and $\delta_{i_o}^c = \arg\Gamma(1-\imath\zeta)$ is the Coulomb phase. Open channels have $p_{i_o}^2 \geqslant 0$, and close channels have $p_{i_o}^2 < 0$. Suppose that there are $N_o \leqslant N$ open channels, i.e. $p_{i_o}^2 \geqslant 0$ for $i_o = 1, \ldots, N_o$ and $p_{i_o}^2 < 0$ for $i_o = N_o + 1$,

$\ldots, N$. Using the explicit asymptotic expressions of the matrix elements (35) we get the explicit expression of the coefficients $\phi^{(k)}_{ji_o}$ and $\psi^{(k)}_{ji_o}$ via the number of the state (or of the channel) $i_o = n_o + 1$ and the number of the current equation $j = 1, \ldots, N$. The calculation was performed by the algorithm implemented in MAPLE up to $k_{\max} = 15$. For example, at $N \geqslant i_o + k$ and $k = 0, 1, 2$ such elements take the form

$$
\begin{aligned}
&\phi^{(0)}_{i_o i_o} = 1, \qquad \psi^{(0)}_{i_o i_o} = 0,\\
&\phi^{(1)}_{i_o-1 i_o} = 0, \qquad \psi^{(1)}_{i_o-1 i_o} = \frac{\sqrt{n_o}\sqrt{n_o+|m|}}{\gamma},\\
&\phi^{(1)}_{i_o i_o} = 0, \qquad \psi^{(1)}_{i_o i_o} = -\frac{2n_o+|m|+1}{\gamma},\\
&\phi^{(1)}_{i_o+1 i_o} = 0, \qquad \psi^{(1)}_{i_o+1 i_o} = \frac{\sqrt{n_o+1}\sqrt{n_o+|m|+1}}{\gamma},\\
&\phi^{(2)}_{i_o-2 i_o} = -\sqrt{n_o-1}\sqrt{n_o+|m|-1}\sqrt{n_o}\sqrt{n_o+|m|}\left(\frac{p^2_{i_o}}{2\gamma^2}+\frac{1}{4\gamma}\right),\\
&\psi^{(2)}_{i_o-2 i_o} = 0,\\
&\phi^{(2)}_{i_o-1 i_o} = \sqrt{n_o}\sqrt{n_o+|m|}\left(\frac{p^2_{i_o}(2n_o+|m|)}{\gamma^2}+\frac{1}{2\gamma}\right),\\
&\psi^{(2)}_{i_o-1 i_o} = 0,\\
&\phi^{(2)}_{i_o i_o} = -\frac{p^2_{i_o}(6n_o^2+6n_o+2+|m|(6n_o+3)+|m|^2)}{2\gamma^2}-\frac{2n_o+|m|+1}{2\gamma},\\
&\psi^{(2)}_{i_o i_o} = \frac{Z(2n_o+|m|+1)}{2p^2_{i_o}\gamma},\\
&\phi^{(2)}_{i_o+1 i_o} = \sqrt{n_o+1}\sqrt{n_o+|m|+1}\left(\frac{p^2_{i_o}(2n_o+|m|+2)}{\gamma^2}+\frac{1}{2\gamma}\right),\\
&\psi^{(2)}_{i_o+1 i_o} = 0,\\
&\phi^{(2)}_{i_o+2 i_o} = -\sqrt{n_o+1}\sqrt{n_o+|m|+1}\sqrt{n_o+2}\sqrt{n_o+|m|+2}\left(\frac{p^2_{i_o}}{2\gamma^2}-\frac{1}{4\gamma}\right),\\
&\psi^{(2)}_{i_o+2 i_o} = 0.
\end{aligned}
\tag{61}
$$

In addition, one should mention that at large r the linearly independent function (54) satisfy the Wronskian-type relation

$$
\mathbf{Wr}\big(\mathbf{Q}(r); \boldsymbol{\chi}^*(r), \boldsymbol{\chi}(r)\big) = \frac{\imath}{2}\mathbf{I}_{oo}, \tag{62}
$$

where $\mathbf{Wr}(\bullet; a(r), b(r))$ is a generalized Wronskian with a long derivative defined as

$$
\mathbf{Wr}\big(\bullet; a(r), b(r)\big) = r^2\left[a^{\mathrm{T}}(r)\left(\frac{db(r)}{dr} - \bullet\, b(r)\right) - \left(\frac{da(r)}{dr} - \bullet\, a(r)\right)^{\mathrm{T}} b(r)\right]. \tag{63}
$$

Here "*" denotes the complex conjugate and $\mathbf{I}_{oo}$ is the unit matrix of dimension $N_o \times N_o$. These relations will be used to examine the desirable accuracy of the above expansion. Note, that in each kth order, recurrences (57) and (58) include implicitly only the factor Z/p_{i_o}. Expansion (55) holds for $r_{\max} \gg \max(|Z/p_{i_o}|, (2i_o + |m| - 1))/\sqrt{\gamma}$.

4. Description of the POTHMF program

In order to solve radial bound state or scattering problem one needs to calculate radial matrix elements on interval $\Delta = [r_{\min}, r_{\max}]$. The POTHMF program calculates potential matrix elements (12) in Gaussian–Legendre nodes of order $k + 1$ in each subinterval $\Delta_j = [r_{j-1}, r_j]$ where $\Delta = \bigcup_{j=1}^{n} \Delta_j$. In each subinterval Δ_j the nodes of a finite-elements grid are determined by

$$
r^k_{j,i} = r_{j-1} + \frac{h_j}{k} i, \qquad h_j = r_j - r_{j-1}, \quad i = \overline{0,k}, \tag{64}
$$

where k order of finite-element shape functions (interpolating Lagrange polynomials) of the radial solution $\chi(r)$. Dipole matrix elements (38)–(39) are calculated in nodes (64), because of they are multiplied by $\chi(r)$ given the same nodes in calculation of integral (75)–(76).

Note, that potential curves and matrix elements of radial coupling calculated by the POTHMF program can be used for solving bound state and scattering problems using appropriate programs from CPC or other available program libraries. In this paper, we use the finite-element KANTBP program [26] to solve the above mentioned problems.

Fig. 5 presents a flow diagram for the POTHMF program. The function of each subroutine is described in Section 5. The POTHMF program is called from the main routine (supplied by a user) which sets dimensions of the arrays and is responsible for the input data. In the present code each array declarator is written in terms of the symbolic names of constants. These constants are defined in the following PARAMETER statement in the main routine:

PARAMETER (MTOT=600 000,MITOT=70 000,NMESH1=7)

where

- MTOT is the dimension of the working DOUBLE PRECISION array TOT.
- MITOT is the dimension of the working INTEGER array ITOT.
- NMESH1 is the dimension of the DOUBLE PRECISION array RMESH containing the information about the subdivision of the adial interval $[r_{\min}, r_{\max}]$ on subintervals and number of elements on each one of them. NMESH1 is always odd and $\geqslant 3$.

A more concrete assignment of these dimensions is discussed below. In order to change the dimensions of the code, all one has to do is to modify the single PARAMETER statement defined above in the main program unit.

The calling sequence for the subroutine POTHMF is:

```
 CALL POTHMF(TITLE,IMATRX,IDIPOL,IFUNAS,WC,CHARGE,MDIM,NPOL,
1            SHIFTS,TOT,MTOT,ITOT,MITOT,IPRINT,IPRSTP,RMESH,
2            NMESHL,IPARTL,MQNL,POTENL,IOUPL,
3            NMESHR,IPARTR,MQNR,POTENR,IOUPR,
4            FNOUTP,IOUTP,DIPOLD,IOUDD,WFUNAS,IOUWF)
```

Input data

TITLE	CHARACTER	title of the run to be printed on the output listing. The title should be no longer than 70 characters.
IMATRX	INTEGER	flag for performing the calculation of the potential matrix elements: = 0—calculation of potential matrices elements is not carried out; = 1—calculation of potential matrices elements is carried out only for the first atomic state, i.e. for continuum state; = 2—calculation of potential matrices elements is carried out only for the second atomic state, i.e. for bound state; = 3—calculation of potential matrices elements is carried out for both atomic states.
IDIPOL	INTEGER	flag for performing the calculation of the longitudinal/transversal dipole matrix elements: = 0—calculation of longitudinal/transversal dipole matrix elements is not carried out; = 1—calculation of longitudinal/transversal dipole matrix elements is carried out, i.e. between first and second atomic states.
IFUNAS	INTEGER	flag for performing the calculation of the asymptotic matrix solutions of the scattering problem: < 0—calculation of asymptotic matrix solutions is not carried out; $\geqslant 0$ and $\leqslant 15$—calculation of regular and irregular asymptotic solutions and their derivatives are carried out with order IFUNAS at RMESH(NMESHL).
WC	REAL*8	cyclotron frequency > 0.
CHARGE	REAL*8	nuclear charge.
MDIM	INTEGER	number of coupled differential equations.
NPOL	INTEGER	order of finite-element shape functions (interpolating Lagrange polynomials). Usually set to 6. This is parameter corresponding to a number of nodes k of subinterval (64) using in KANTBP program [26]. In case of NPOL = 0 POTHMF program calculates the matrix elements in the endpoints of subintervals and user cannot use KANTBP program [26].

SHIFTS	REAL*8	SHIFTS contains the given double energy spectrum value $\varepsilon = 2E$ (in a.u.) for scattering problem. This value should be greater than the first threshold and not equals to the open threshold values $\epsilon_{mj}^{th}(\gamma)$ from (36). Else the message about an error is printed and the execution of the program is aborted. The number of open channels N_o is calculated in the program by formula $1 \leqslant N_o = \max_{2E>\epsilon_{mj}^{th}} j < N$.
IPRINT	INTEGER	level of print: $= 0$—minimal level of print. The initial data, short information about the numerical scheme parameters, main flags and keys are printed out; $= 1$—matrix elements calculated are printed out in corresponding point r with step IPRSTP additionally; $= 2$—optimal numbers $N_{\max}$ of the terms of expansion (17) calculated by the algorithm (50) are printed out in corresponding point r with step IPRSTP additionally.
IPRSTP	INTEGER	step with which the calculated matrix elements are printed out.
RMESH	REAL*8	array RMESH contains information about subdivision of interval $[r_{\min}, r_{\max}]$ of radius r on subintervals. The whole interval $[r_{\min}, r_{\max}]$ is divided as follows: RMESH(1) $= r_{\min}$, RMESH(NMESHL) $= r_{\max}$, and the values of RMESH(I) set the number of elements for each subinterval [RMESH(I-1), RMESH(I+1)], where $I = 2, 4, \ldots,$ NMESHL–1.
NMESHL NMESHR	INTEGER	dimensions of array RMESH of the first and second atomic states, respectively. For the calculation of longitudinal/transversal dipole matrix elements used NMESHR. These dimensions always should be odd and NMESHL $\geqslant$ NMESHR $\geqslant 3$.
IPARTL IPARTR	INTEGER	parities of the first and second atomic states calculated by formula $(1 - \sigma)/2$, respectively: $= 0$, for even parity; $= 1$, for odd parity.
MQNL MQNR	INTEGER	magnetic quantum numbers of the first and second atomic states, respectively.
POTENL POTENR	CHARACTER	names of the output files (up to 55 characters) containing potential matrix elements of radial coupling for first and second atomic states calculated for a Gaussian nodes from the interval [RMESH(1),RMESH(NMESHL)] and [RMESH(1),RMESH(NMESHR)], respectively.
IOUPL IOUPR	INTEGER	number of the logical device for storing data into files POTENL and POTENR, respectively.
FNOUTP	CHARACTER	name of the output file (up to 55 characters) for printing out the results of the calculation. It is system specific and may include a complete path to the file location.
IOUTP	INTEGER	number of the output logical device for printing out the results of the calculation (usually set to 7).
DIPOLD	CHARACTER	name of the output file (up to 55 characters) containing longitudinal/transversal dipole matrix elements of radial coupling for first and second atomic states calculated for a given set of radial points from the interval [RMESH(1),RMESH(NMESHR)].
IOUDD	INTEGER	number of the logical device for storing data into file DIPOLD.
WFUNAS	CHARACTER	name of the output file (up to 55 characters) containing regular and irregular asymptotic solutions and their derivatives for the scattering problem.
IOUWF	INTEGER	number of the logical device for writing data from file WFUNAS.
TOT	REAL*8	working vector of the DOUBLE PRECISION type.
ITOT	INTEGER	working vector of the INTEGER type.
MTOT	INTEGER	dimension of the DOUBLE PRECISION working array ITOT. The last address ILAST of array TOT is calculated and then compared with the given value of MTOT. If ILAST > MTOT the message about an error is printed and the execution of the program is aborted. In the last case, in order to carry out the required calculation it is necessary to increase the dimension MTOT of array TOT to the ILAST value taken from the message.

MITOT	INTEGER	dimension of the INTEGER working array ITOT. The last address ILAST of array ITOT is calculated and then compared with the given value of MITOT. If ILAST > MITOT the message about an error is printed and the execution of the program is aborted. In the last case, in order to carry out the required calculation it is necessary to increase the dimension MITOT of array ITOT to the ILAST value taken from the message.

Output data

The results of the calculation of potential matrix elements in the Gauss–Legendre nodes from the interval [RMESH(1), RMESH(NMESHL/NMESHR)] are written using unformatted segmented records into file POTENL/POTENR with number IOUP (IOUPL/IOUPR), according to the following operator:

```
 WRITE(IOUP) L,(((UPOT(I,J,IG),J=I,MDIM),I=1,MDIM),IG=1,NGQ),
1               (((QPOT(I,J,IG),J=I+1,MDIM),I=1,MDIM),IG=1,NGQ)
```

The results of the calculation of potential matrix elements in the RMESH (NMESHL / NMESHR) are written using unformatted segmented records into the above file, according to the following operator:

```
 WRITE(IOUP) NGRID,((H(I,J),J=I,MDIM),I=1,MDIM),
1                  ((Q(I,J),J=I+1,MDIM),I=1,MDIM)
```

The results of the calculation of longitudinal/transversal dipole matrix elements for the given set of radial points from the interval [RMESH(1),RMESH (NMESHR)] are written using unformatted segmented records into file DIPOLE with number IOUDD, according to the following operator:

```
WRITE(IOUDD) IG,((DD(I,J),J=1,MDIM),I=1,MDIM)
```

The results of the calculation of regular and irregular asymptotic matrix-solutions and their derivatives are written using unformatted segmented records into file WFUNAS with number IOUWF, according to the following operator:

```
 WRITE(IOUWF) MDIM,NOPEN,(QR(I),I=1,NOPEN),
1                        (( PREG(I,J),J=1,NOPEN),I=1,MDIM),
2                        (( PIRR(I,J),J=1,NOPEN),I=1,MDIM),
3                        ((DPREG(I,J),J=1,NOPEN),I=1,MDIM),
4                        ((DPIRR(I,J),J=1,NOPEN),I=1,MDIM)
```

In the above, parameters presented in the WRITE statement have the following meaning:

- L is number of finite element.
- NGRID is the number of grid points.
- IG is the number of grid point.
- NGQ = NPOL + 1.
- NOPEN is the number of open channels.
- Arrays UPOT and QPOT contain the potential matrices values calculated.
- Array DD contains the longitudinal/transversal dipole matrix values calculated.
- Array QR contains the values of the momentums, QR(J) = $\sqrt{2E - \epsilon^{th}_{mj}(\gamma)}$.
- Arrays PREG, PIRR and DPREG, DPIRR contain the values of the regular and irregular asymptotic matrix-solutions and their derivatives, respectively.

5. Description of subprogram units

A flow diagram for the POTHMF program is presented in Fig. 5. The function of each subroutine is briefly described below. Additional details may be found in COMMENT cards within the program.

- Subroutine ERRMDM prints error messages when high-speed storage requested by a user is exceeded and stops the execution of program POTHMF.
- Subroutine GAULEG [39] calculates nodes and weights of the Gauss–Legendre quadrature. This subroutine is included in main body program.

- Subroutine FEGRID [26] calculates nodal points for the finite-element uniform grid. This subroutine is included in main body program.
- Subroutine HQPOTM calculates the potential matrix elements $\mathbf{V}(r)$, $\mathbf{Q}(r)$ of dimension MDIM × MDIM of radial coupling in the Gaussian nodes and storing using unformatted segmented records into file POTEN.
- Subroutine MAGNET calculates the potential matrix elements $\mathbf{V}(r)$, $\mathbf{Q}(r)$ of dimension MDIM × MDIM.
- Subroutine SPECTR evaluates the potential matrix elements $\mathbf{H}(r)$, $\mathbf{Q}(r)$ of dimension MDIM × MDIM and the potential curves $\boldsymbol{\varepsilon}(r)$ of dimension MDIM calculated via solutions of the algebraic problems (19) and (25) of dimension $N_{\max} \times N_{\max}$.
- INTEGER function NOPTIM calculates the optimal number $N_{\max}$ for the calculation of the algebraic eigenvalue problem (19) with the relative machine precision.
- Subroutine SOLUTN solves the algebraic eigenvalue problem (19) and sets of inhomogeneous algebraic equations (25).
- DOUBLE PRECISION function AMKANT prepares matrix $\mathbf{A}^{(0)}$ in the eigenvalue problem (19) and its derivatives.
- DOUBLE PRECISION function SIN2 prepares coefficients of p^2 of matrix $\mathbf{A}^{(0)}$ in the eigenvalue problem (19).
- Subroutine DSTEVR [33] solves the first MDIM eigenvalues and corresponding eigenvectors of the algebraic eigenvalue problem for the real symmetric tridiagonal matrix.
- Subroutine DBANDM calculates $\mathbf{LDL}^{\mathrm{T}}$ factorization of the tridiagonal matrix. This factorization is used in subroutine DPTTRS.
- Subroutine DPTTRS [33] solves sets of inhomogeneous algebraic equations for the real symmetric tridiagonal matrix.
- DOUBLE PRECISION function QASINF calculates the terms of the potential matrix elements $\mathbf{Q}(r)$ in expansion (35).
- DOUBLE PRECISION function HASINF calculates the terms of the potential matrix elements $\mathbf{H}(r)$ in expansion (35).
- DOUBLE PRECISION function SPEINF calculates the terms of the potential curve $\boldsymbol{\varepsilon}(r)$ in expansion (35).
- Subroutine DIPPOT calculates the longitudinal/transversal dipole matrices elements $\mathbf{D}^{(m\sigma\sigma')}(r)/\mathbf{P}^{(mm'\sigma)}(r)$ of dimension MDIM × MDIM of radial coupling in the given set of radial points and stores them using unformatted segmented records into file DIPOLD.
- Subroutine DIPOLE evaluates the longitudinal dipole matrix elements $\mathbf{D}^{(m\sigma\sigma')}(r)$ of dimension MDIM × MDIM.
- Subroutine SPECTD evaluates the longitudinal dipole matrix elements $\mathbf{D}^{(m-1+1)}(r)$ of dimension MDIM × MDIM calculated via solutions of the algebraic eigenvalue problem (19) of dimension $N_{\max} \times N_{\max}$.
- DOUBLE PRECISION function DASINF calculates the terms of the longitudinal dipole matrix elements $\mathbf{D}^{(m\sigma\sigma')}(r)$ of expansion (42).
- Subroutine CPOLAR evaluates the transversal dipole matrix elements $\mathbf{P}^{(mm'\sigma)}(r)$ of dimension MDIM × MDIM.
- Subroutine SPECTP evaluates the transversal dipole matrix elements $\mathbf{P}^{(m_<m_>\sigma)}(r)$ at $m_< = \min(|m|, |m'|)$, $m_> = \max(|m|, |m'|)$ of dimension MDIM × MDIM calculated via solutions of the algebraic eigenvalue problem (19) of dimension $N_{\max} \times N_{\max}$.
- DOUBLE PRECISION function CASINF calculates the terms of the transversal dipole matrix elements $\mathbf{P}^{(m_<m_>\sigma)}(r)$ of expansion (42).
- Subroutine ASYMFN calculates the regular and irregular asymptotic matrix-solutions $\boldsymbol{\chi}^s(r)$, $\boldsymbol{\chi}^c(r)$ and their derivatives and writes them using unformatted segmented records into file WFUNAS. Also this subroutine calculates the generalized Wronskian relation by the formula (69) using DOUBLE PRECISION function QASINF.
- Subroutine MAGASC calculates the regular and irregular asymptotic matrix-solutions $\boldsymbol{\chi}^s(r)$, $\boldsymbol{\chi}^c(r)$ and their derivatives of the scattering problem.
- Subroutine FUNINF calculates of terms of expansion (54), (55) of asymptotics of regular and irregular solutions and their derivatives and prints a message about recommended right bound of interval $r_{\max}$ and value of the matching point r_{match} from Eq. (52) with the given accuracy $eps_c = 10^{-14}$.
- Subroutine RCWFNN calculates the Coulomb regular and irregular solutions and their derivatives with the given accuracy $eps_c = 10^{-14}$. This subroutine is the modified version of the subroutine RCWFN [40] for DOUBLE PRECISION type. This subroutine is included in main body program.

6. Test desk

The test run which accompanies the POTHMF program computes the potential and longitudinal dipole matrix elements for the given atomic states (for the initial state $\sigma = +1$ and for the final state $\sigma = -1$) with $Z = 1$, $\gamma = 1$ and $m = 0$. After that, we applied the calculated matrix elements to the calculation of the ground state energy and reaction matrix for initial and final atomic states with help of the KANTBP program [26], respectively.

File 'INITIAL.INP' contains the initial data NAMELIST POTDAT for the calculation of the potential and longitudinal dipole matrix elements for the given atomic states for the POTHMF program. Also this file contains the initial data NAMELIST PARDIS and NAMELIST PARSCP for the calculation of the ground state energy and reaction matrix for the KANTBP program (see details in [26]), respectively. File 'INITIAL.INP' contains the following data:

```
&POTDAT TITLE=' Potential and dipole matrices elements ',
        IMATRX=3,IDIPOL=1,IFUNAS=15,WC=0.1D1,CHARGE=1.D0,MDIM=6,
        NPOL=4,SHIFTS=3.4D0,IPRINT=1,IPRSTP=1501,
        RMESH=0.0D0,200.D0,3.D0,200.D0,20.D0,200.D0,100.D0,
        FNOUTP='FNOUTP.LPR',IOUTP=7,
        NMESHL=7,IPARTL=1,MQNL=0,POTENL='POTENL.PTN',IOUPL=8,
        NMESHR=7,IPARTR=0,MQNR=0,POTENR='POTENR.PTN',IOUPR=9,
        DIPOLD='DIPOLP.PTN',IOUDD=10,WFUNAS='WFUNAS.PTN',IOUWF=1
&END
&PARDIS TITLE1=' Bound state energy levels ',
        IPTYPE=0,NROOT=1,IDIM=3,RTOL=1.D-15,
        NITEM=150,SHIFT=-0.7D0,IPRINT=2,IPRSTP=480,
        NDIR=1, NDIL=6, NMDIL=1,IBOUND=3,
        FNOUTR='3DNSAS.LPR',IOUT=11,FMATRR='3DNSAS.MAT',IOUM=12,
        EVWFNR='3DNSAS.WFN',IOUF=0
&END
&PARSCP TITLE2=' Reaction matrix ',
        IPTYPE=1,NROOT=1,SHIFT=3.4D0,IPRINT=2,IPRSTP=480,IBOUND=8,
        THRSHL=1.D0,3.D0,5.D0,7.D0,9.D0,11.D0,
        FNOUTL='3DNSSC.LPR',NOUT=14,FMATRL='3DNSSC.MAT',NOUM=15,
        EVWFNL='3DNSSC.WFN',NOUF=0
&END
```

Physical parameters CHARGE, WC, MQNL and order of asymptotic solutions IFUNAS are accessed via general common block COMMON /CHARGE/ CHARGE, WC, MQNL, IFUNAS. The user subroutine ASYMSC should contain this common block and could be written as follows:

```
      SUBROUTINE ASYMSC(RMAX,NDIM,NOPEN,QR,PREG,PIRR,DREG,DIRR,IOUT)
C . . . . . . . . . . . . . . . . . . . . . . . . . . . . . . . . .
C .                                                               .
C .   P R O G R A M                                             .
C .                TO CALCULATE THE REGULAR, IRREGULAR           .
C .                ASYMPTOTIC MATRIX SOLUTIONS PREG, PIRR        .
C .                AND THEIR DERIVATIVES DREG, DIRR AT RMAX      .
C .                                                               .
C . . . . . . . . . . . . . . . . . . . . . . . . . . . . . . . . .
      IMPLICIT REAL*8 (A-H,O-Z)
      PARAMETER (NWOR=3000)
      DIMENSION QR(NOPEN),PREG(NDIM,NOPEN),PIRR(NDIM,NOPEN),
     1          DREG(NDIM,NOPEN),DIRR(NDIM,NOPEN)
      DIMENSION WORK(NWOR)
      COMMON /CHARGE/ CHARGE,WC,MQNL,IFUNAS
      CALL MAGASC(RMAX,NDIM,NOPEN,QR,PREG,PIRR,DREG,DIRR,IFUNAS,
     1            WORK,NWOR,CHARGE,WC,MQNL,IOUT)
      RETURN
      END
```

The test run which accompanies this paper took 7 s for calculation of potential curves, matrix elements and dipole transition matrix elements, and 2 s for calculation of discrete and continuous spectrum problems using the obtained potential curves and matrix elements on the Intel Pentium IV 2.4 GHz, respectively. The potential curves $\varepsilon_j(r)$, matrix elements $Q_{ij}(r)$, $H_{ij}(r)$, longitudinal dipole matrix elements $D_{ij}^{(m\sigma\sigma')}(r)$ and corresponding wave functions of continuum spectrum of this test run are presented in Figs. 1–4, 6. The finite element grid in r has been chosen as 0 (200) 3 (200) 20 (200) 100 from the initial data list (see description of array RMESH). The numbers in parentheses are the numbers of finite elements of order $k = 4$ on each subinterval (see description value NPOL).

7. Benchmark calculations of the photoionization cross-sections

In this section we present calculation of photoionization cross-sections with the help of the KANTBP program using potential curves, radial matrix elements and dipole matrix elements computed by the POTHMF program. Eigenfunction of the continuum spectrum $\Psi_i^{Em\sigma}(r,\eta)$ with the energy $\epsilon = 2E$ describing the ejected electron above the first threshold $\epsilon_{m1}^{th}(\gamma) = \gamma(|m| + m + 1)$ is

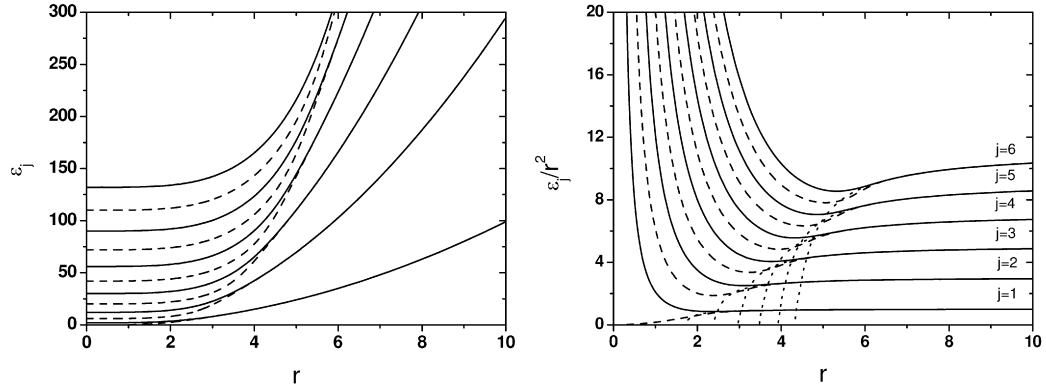

Fig. 1. Potential curves $\varepsilon_j(r)$, at $m = 0$ and $\gamma = 1$. Full line—odd state; dashed line—even state. Dotted lines display the asymptotic behavior at large r.

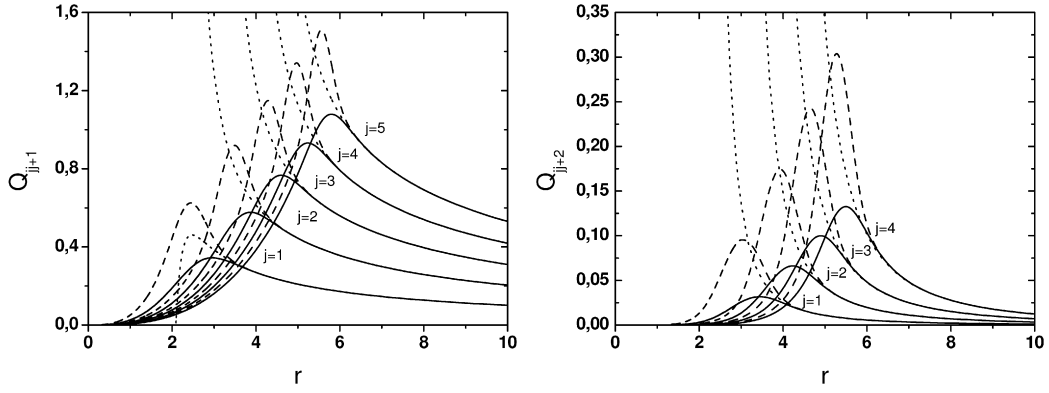

Fig. 2. Radial matrix elements $Q_{jj+1}(r)$, $Q_{jj+2}(r)$ at $m = 0$ and $\gamma = 1$. Full line—odd state; dashed line—even state. Dotted lines display the asymptotic behavior at large r.

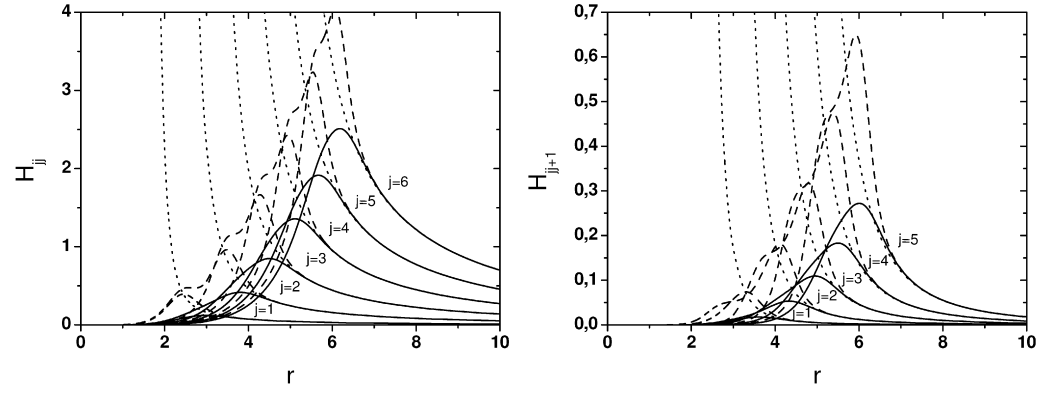

Fig. 3. Radial matrix elements $H_{jj}(r)$, $H_{jj+1}(r)$ at $m = 0$ and $\gamma = 1$. Full line—odd state; dashed line—even state. Dotted lines display the asymptotic behavior at large r.

expressed as follows:

$$\Psi_i^{Em\sigma}(r,\eta) = \sum_{j=1}^{N} \Phi_j^{m\sigma}(\eta;r)\hat{\chi}_{ji}^{(m\sigma)}(E,r), \quad i = 1,\ldots,N_o, \tag{65}$$

where solution $\hat{\boldsymbol{\chi}}^{(m\sigma)}(E,r)$ is the radial part of the "incoming" or eigenchannel wave function. In this case the eigenfunction $\Psi_i^{Em\sigma}(r,\eta)$ is normalized by

$$\begin{aligned}\left\langle \Psi_i^{Em\sigma}(r,\eta) \middle| \Psi_{i'}^{E'm'\sigma'}(r,\eta) \right\rangle &= \sum_{j=1}^{N} \int_0^{\infty} r^2\, dr \left(\hat{\chi}_{ji}^{(m\sigma)}(E,r)\right)^* \hat{\chi}_{ji'}^{(m'\sigma')}(E',r) \\ &= \delta(E-E')\delta_{mm'}\delta_{\sigma\sigma'}\delta_{ii'}. \end{aligned} \tag{66}$$

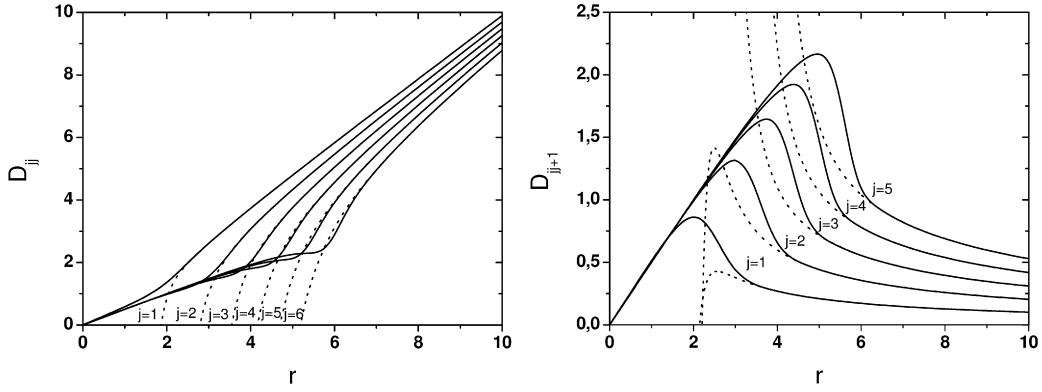

Fig. 4. Longitudinal dipole matrix elements $D_{jj}^{(m\sigma\sigma')}(r)$, $D_{jj+1}^{(m\sigma\sigma')}(r)$ at $m=0$, $\sigma=-1$, $\sigma'=1$ and $\gamma=1$. Dotted lines display the asymptotic behavior at large r.

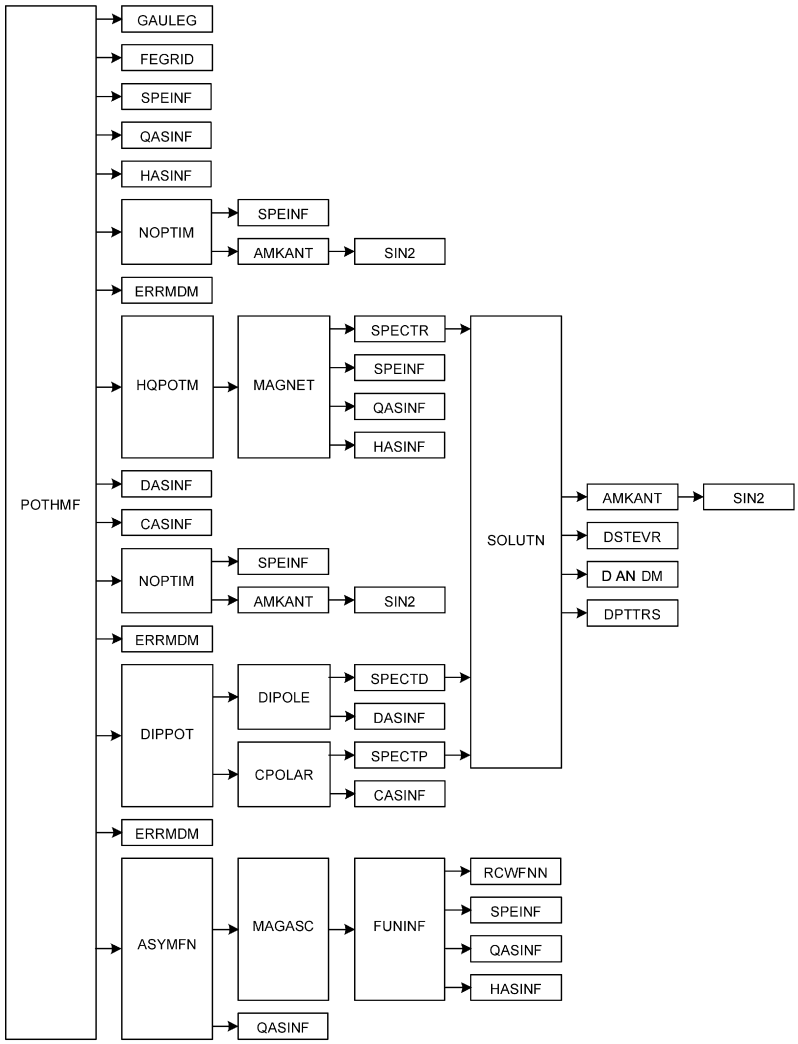

Fig. 5. Flow diagram of the POTHMF program.

The radial eigenchannel function $\hat{\chi}^{(m\sigma)}(E,r)$ is calculated by formula

$$\hat{\chi}^{(m\sigma)}(E,r)=\sqrt{\frac{2}{\pi}}\chi^{(p)}(r)\mathbf{B}\cos\delta. \tag{67}$$

Here, $\chi^{(p)}(r)$ is the numerical solution of Eq. (11) that satisfies the "standing" wave boundary conditions (15) and has the standard asymptotic form [26]

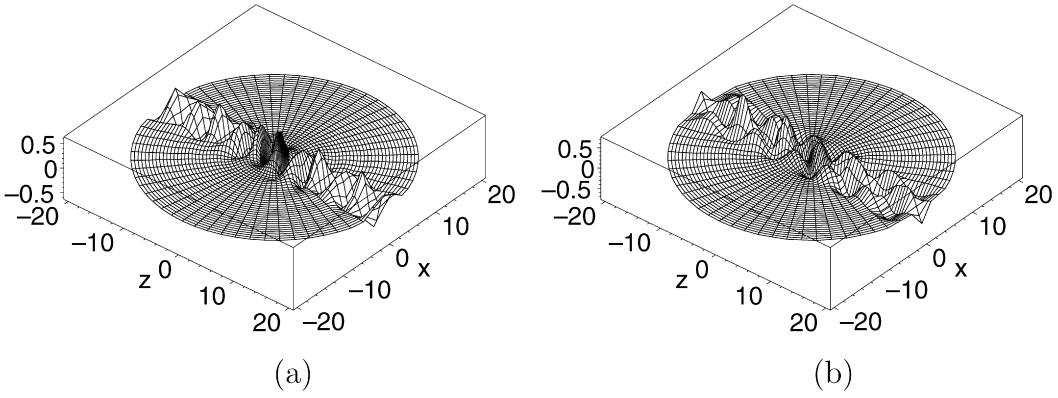

Fig. 6. The wave functions Ψ_1 and Ψ_2 of the first (a) and second (b) open channels of the continuum spectrum states having asymptotic (67) in the zx plane for $\sigma = -1$, $Z = 1$, $\gamma = 1$ and $m = 0$ with energy $E = 1.7$ a.u. above the second threshold $1/2\epsilon_{m2}^{th} = 1.5$.

$$\boldsymbol{\chi}^{(p)}(r) = \boldsymbol{\chi}^{s}(r) + \boldsymbol{\chi}^{c}(r)\mathbf{K}, \qquad \mathbf{K}\mathbf{B} = \mathbf{B}\tan\boldsymbol{\delta}, \qquad \mathbf{B}\mathbf{B}^{\mathrm{T}} = \mathbf{B}^{\mathrm{T}}\mathbf{B} = \mathbf{I}_{oo}, \tag{68}$$

where $\boldsymbol{\chi}^{s}(r) = 2\Im(\boldsymbol{\chi}(r))$ and $\boldsymbol{\chi}^{c}(r) = 2\Re(\boldsymbol{\chi}(r))$, $\mathbf{K}$ is the numerical short-range reaction matrix, $\tan\boldsymbol{\delta}$ and $\mathbf{B}$ are the eigenvalue and the orthogonal matrix of a set of the corresponding eigenvectors. In the latter the regular and irregular functions satisfy the generalized Wronskian relation (63) at large r

$$\mathbf{Wr}\big(\mathbf{Q}(r);\, \boldsymbol{\chi}^{c}(r), \boldsymbol{\chi}^{s}(r)\big) = \mathbf{I}_{oo}. \tag{69}$$

The radial part of the "incoming" wave function is expressed via the numerical "standing" wave function and short-range reaction matrix $\mathbf{K}$ by the relation

$$\hat{\boldsymbol{\chi}}^{(m\sigma)}(E, r) = \sqrt{\frac{2}{\pi}}\boldsymbol{\chi}^{-}(r) = \imath\sqrt{\frac{2}{\pi}}\boldsymbol{\chi}^{(p)}(r)(\mathbf{I}_{oo} + \imath\mathbf{K})^{-1} \tag{70}$$

and has the asymptotic form

$$\hat{\boldsymbol{\chi}}^{(m\sigma)}(E, r) = \sqrt{\frac{2}{\pi}}\big(\boldsymbol{\chi}(r) - \boldsymbol{\chi}^{*}(r)\mathbf{S}^{\dagger}\big), \tag{71}$$

where $\mathbf{S}$ is the short-range scattering matrix and

$$\mathbf{S}^{\dagger}\mathbf{S} = \mathbf{S}\mathbf{S}^{\dagger} = \mathbf{I}_{oo}, \qquad \mathbf{K} = \imath(\mathbf{I}_{oo} + \mathbf{S})^{-1}(\mathbf{I}_{oo} - \mathbf{S}), \qquad \mathbf{S} = (\mathbf{I}_{oo} + \imath\,\mathbf{K})(\mathbf{I}_{oo} - \imath\mathbf{K})^{-1}. \tag{72}$$

The total wave function having the asymptotic form "waves going into the center + outgoing wave" [28],

$$\boldsymbol{\Psi}^{(-)}_{Em\overrightarrow{\leftarrow}}(r, \eta) = \frac{\boldsymbol{\Psi}^{Em\sigma=+1}(r, \eta) \pm \boldsymbol{\Psi}^{Em\sigma=-1}(r, \eta)}{\sqrt{2}}\exp(-\imath\boldsymbol{\delta}^{c}). \tag{73}$$

In terms of the above definitions the cross section of photoionization $\sigma^{d}_{m\sigma\sigma'}(\omega)$ by the light linearly polarized along z-axis and $\sigma^{p}_{mm'\sigma}(\omega)$ by the light circularly polarized in the plane XOY are expressed as

$$\sigma^{d}_{m\sigma\sigma'}(\omega) = C\omega\sum_{i=1}^{N_o}\big|\hat{D}^{m\sigma\sigma'}_{i,i',\nu'}(E)\big|^2, \qquad \sigma^{p}_{mm'\sigma}(\omega) = C\omega\sum_{i=1}^{N_o}\big|\hat{P}^{mm'\sigma}_{i,i',\nu'}(E)\big|^2. \tag{74}$$

Here $\hat{D}^{m\sigma\sigma'}_{i,i',\nu'}(E)$ and $\hat{P}^{mm'\sigma}_{i,i',\nu'}(E)$ are the matrix elements of the longitudinal and transversal dipole moment, respectively:

$$\begin{aligned}\hat{D}^{m\sigma\sigma'}_{i,i',\nu'}(E) &= \big\langle\Psi_i^{Em\sigma}(r, \eta)\big|r\eta\big|\Psi^{m'=m,\sigma'=-\sigma}_{i'\nu'}(r, \eta)\big\rangle \\ &= \sum_{j=1}^{N}\sum_{j'=1}^{N}\int_0^{r_{\max}} r^2\,dr\big(\hat{\chi}^{(m\sigma)}_{ji}(E, r)\big)^{*}D^{(m\sigma\sigma')}_{jj'}(r)\chi^{(m'=m,\sigma'=-\sigma)}_{j'i'\nu'}(r),\end{aligned} \tag{75}$$

$$\begin{aligned}\hat{P}^{mm'\sigma}_{i,i',\nu'}(E) &= \left\langle\Psi_i^{Em\sigma}(r, \eta)\left|r\frac{\sqrt{1-\eta^2}}{\sqrt{2}}\right|\Psi^{m'=m\pm1,\sigma'=\sigma}_{i'\nu'}(r, \eta)\right\rangle \\ &= \sum_{j=1}^{N}\sum_{j'=1}^{N}\int_0^{r_{\max}} r^2\,dr\big(\hat{\chi}^{(m\sigma)}_{ji}(E, r)\big)^{*}P^{(mm'\sigma)}_{jj'}(r)\chi^{(m'=m\pm1,\sigma'=\sigma)}_{j'i'\nu'}(r),\end{aligned} \tag{76}$$

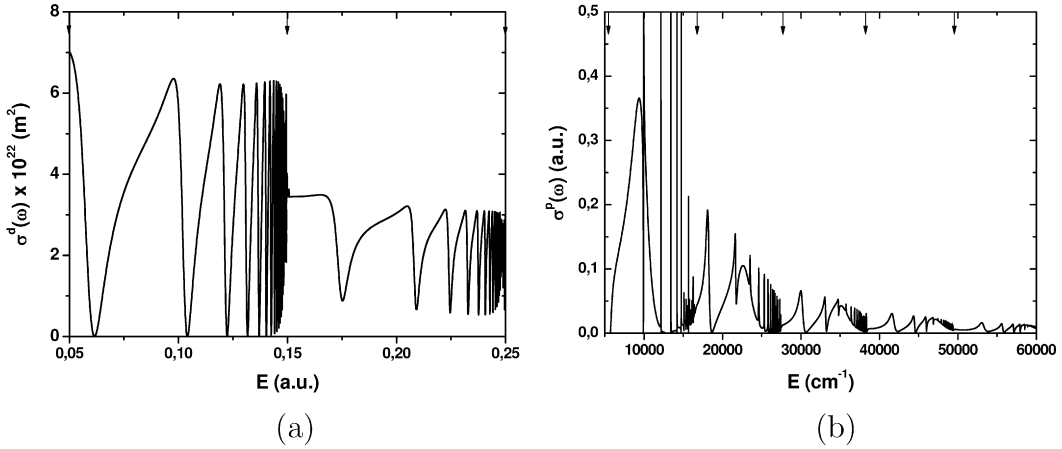

Fig. 7. Photoionization cross-sections $\sigma^d_{m\sigma\sigma'}(\omega)$ (a) and $\sigma^p_{mm'\sigma}(\omega)$ (b). (a) The photoionization is from the ground state $1s_0$ with $\gamma = 0.1$, $\sigma' = 1$ and $m = 0$ to final state with $\sigma = -1$. (b) The photoionization is from the excited state $2p_{-1}$ with $\gamma = 0.05$, $\sigma = 1$ and $m' = -1$ to final state with $m = 0$. The arrows indicate the successive Landau thresholds $1/2\epsilon^{th}_{mj}$ from (35), where j runs from 1 to 2 in (a) and runs from 1 to 5 in (b).

where longitudinal $\mathbf{D}^{(m\sigma\sigma')}(r)$ and transversal $\mathbf{P}^{(mm'\sigma)}(r)$ dipole matrix elements are calculated by formulae (38) and (39). The cross sections (74) in terms of the $\hat{D}^{m\sigma\sigma'}_{i,i',\nu'}(\hat{E})$ and $\hat{P}^{mm'\sigma}_{i,i',\nu'}(\hat{E})$ expressed via $\mathbf{D}^{(m\sigma\sigma')}(\hat{r})$ and transversal $\mathbf{P}^{(mm'\sigma)}(\hat{r})$ in scaled variable $\hat{r}$ and the parameters $\hat{E}$, $\hat{Z}$ reads as

$$\sigma^d_{m\sigma\sigma'}(\omega) = \frac{C\omega}{\gamma^2}\sum_{i=1}^{N_o}\left|\hat{D}^{m\sigma\sigma'}_{i,i',\nu'}(\hat{E})\right|^2, \qquad \sigma^p_{mm'\sigma}(\omega) = \frac{C\omega}{\gamma^2}\sum_{i=1}^{N_o}\left|\hat{P}^{mm'\sigma}_{i,i',\nu'}(\hat{E})\right|^2. \tag{77}$$

In the above expressions, $\omega = E - E_{m'\sigma'i'\nu'}$ is the frequency of radiation, $E_{nlm} \equiv E_{m'\sigma'i'\nu'} < \epsilon^{th}_{mi'}(\gamma)/2$ is the energy of the initial bound state $\Psi^{m'\sigma'}_{i',\nu'}(r,\eta)$ with $i' = 1$ and vibration number $\nu' = 0, 1, \ldots, N-1$, E is the energy of the final continuum state $\Psi^{Em\sigma}_i(r,\eta)$ such that N_o is the number of the open channels, $C = 4\pi^2\alpha a_0^2$ is a constant, α is the fine-structure constant, and a_0 is the Bohr radius. The continuum spectrum solution $\boldsymbol{\chi}^{(p)}(r)$ having asymptotic of "standing" wave conditions and reaction matrix $\mathbf{K}$ required for calculation of (67) or (71), and discrete spectrum solution $\boldsymbol{\chi}^{m'\sigma'}_{i'\nu'}(r)$ and eigenvalue $E_{m'\sigma'i'\nu'}$ have been calculated with the help of the program KANTBP [26]. One can see that using (67) or (71) for calculating the absolute value in formula (74) yields the same result. Therefore, (67) is preferable for using real arithmetics. Note, that using physical function constructed via (67) with mixed parity that has an appropriate asymptotic of the incoming wave in cylindrical coordinates on the whole axis z leads to the same result [28].

Fig. 7 displays the photoionization cross-sections $\sigma^d_{m\sigma\sigma'}(\omega)$ and $\sigma^p_{mm'\sigma}(\omega)$ calculated by programs POTHMF and KANTBP. The finite element grids of $\hat{r}$ have been chosen as 0 (200) 3 (200) 20 (200) 100 for the discrete spectrum and 0 (200) 3 (200) 20 (200) 100 (1000) 1000 for the continuum one. The numbers in parentheses are the numbers of finite elements of order $k = 4$ on each interval. In the calculations we have used the following values of physical constants [41]: the Bohr radius $a_0 = 5.29177 \times 10^{-11}$ m, the fine-structure constant $\alpha = 7.29735 \times 10^{-3}$ and 1 cm^{-1} $= 4.55633 \times 10^{-6}$ a.u.

Fig. 7(a) shows the photoionization cross section from the ground state $1s_0$ with $\gamma = 0.1$, $\sigma' = 1$ and $m = 0$ to final state with $\sigma = -1$. The number of open channels is equal to 1 and 2 and dimension of the truncated system (11) is equal to $N = 10$. In the whole energy interval the results are in good agreement with those of **R**-matrix calculations within the MQDT [12]. We also compared our result with those of the complex-rotation method combined with a basic set of the 10 000 complex spherical Sturmian-type expansion (CSSTE) [15] and of the 450 mixed Slater–Landau basis (MSLB) [17]. In this case the agreement is good between the thresholds, but not near them. Fig. 7(b) shows the photoionization cross section from the excited state $2p_{-1}$ with $\gamma = 0.05$, $\sigma = 1$ and $m' = -1$ to final state with $m = 0$. The number of the open channels varied from 1 to 5 and dimension of the truncated system (11) is equal to $N = 18$. We compared our result with those of the complex-rotation method combined with a basic set of the 10 000 CSSTE [16] and of the 288 MSLB [17]. In this case we have the some agreement between the thresholds, but not near them. So, the calculated photoionization cross sections have the true behavior above the thresholds that is one of the goal of the elaborated approach.

Fig. 8(a) displays the cross-section of photoionization by the light linearly polarized along the axis z from the rotational state $3s_0$ at $B_0 = 6.10$ T ($\gamma = 2.595 \times 10^{-5}$) in the energy interval between $E = 6.0$ cm^{-1} and $E = 8.0$ cm^{-1}. In this case we increased N up to 35 and the finite element grids of $\hat{r} = \sqrt{\gamma}r$ were chosen as 0 (200) 0.03 (200) 0.2 (200) 1 for the discrete spectrum and 0 (200) 0.03 (200) 0.2 (200) 1 (2000) 100 (4000) 1000 for the continuous one. The number of nodes in these grids is 2400 and 26 401, respectively. The corresponding maximal number of unknowns in Eqs. (11) is 84 000 and 924 035. Fig. 8(b) shows the absolute maximum values of the continuum wave functions $\hat{\chi}^{(01)}_{j1}(E,\hat{r})$ at $E = 6.0$ cm^{-1}. We calculated the cross-sections with the energy

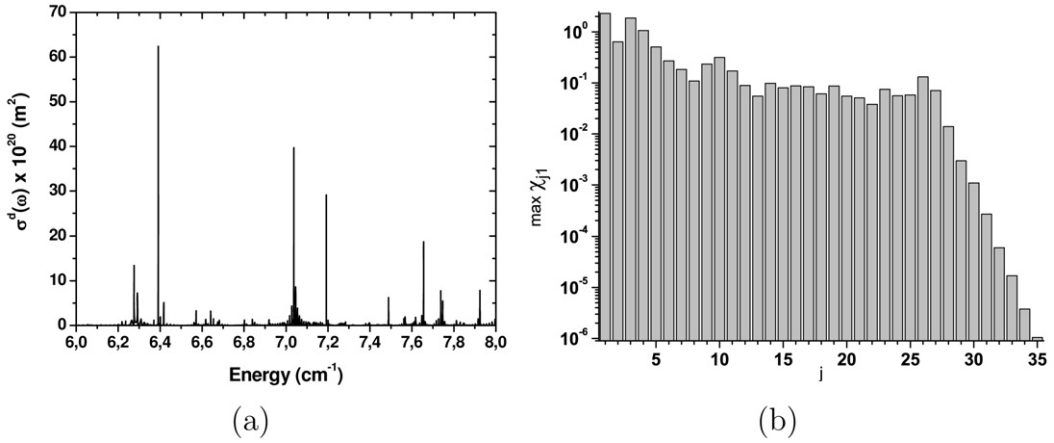

Fig. 8. (a) Cross-section of photoionization from the state $3s_0$ versus the energy for $\gamma = 2.595 \times 10^{-5}$ and for the final state with $\sigma = -1$, $Z = 1$, $m = 0$. (b) Absolute maximum values of the continuum wave functions $\hat{\chi}^{(01)}_{j1}(E, \hat{r})$ at $E = 6.0$ cm^{-1} and $N = 35$ using for calculation in figure (a).

step 5×10^{-4} cm^{-1} in all the region except the vicinity of peaks, where the step was 5×10^{-6} cm^{-1}. Note, that states $3d_0$, $3p_0$ and $3s_0$ with energies $E_{320} = -0.055\,555\,552\,07$ a.u., $E_{310} = -0.055\,555\,549\,49$ a.u. and $E_{300} = -0.055\,555\,542\,37$ a.u., respectively, are nearly degenerate. In this case we have a good agreement [15] used a basic set of the 62 500 CSSTE. More detailed discussion of results of calculation of a hydrogen atom in a strong magnetic field using the POTHMF program for calculating potential curves and matrix elements of radial coupling and dipole matrix elements is given in paper [29] where a good agreement with the results of calculations performed by other methods has been demonstrated.

8. Conclusions

A new efficient method of calculating both discrete and continuum spectrum wave functions of a hydrogen atom in a strong magnetic field is developed based on the Kantorovich approach to the parametric eigenvalue problems in spherical coordinates. The two-dimensional spectral problem for the Schrödinger equation with fixed magnetic quantum number and parity is reduced to a one-dimensional spectral parametric problem for the angular variable and a finite set of ordinary second-order differential equations in the radial variable. The rate of convergence of the method is examined numerically and is illustrated with a number of typical examples. The main advantage of the elaborated approach lies in the fact that calculations on all steps of the Kantorovich approach are realized with the help of stable calculation schemes and with a prescribed accuracy. The economy of computer resources is achieved with the help of calculated asymptotics for a set of adaptive basis functions, matrix elements of radial coupling and radial solutions in analytic form by means of the MAPLE computer algebra algorithms [23]. This allows one to significantly reduce the interval of integration of the corresponding boundary problems. It is shown that the calculated photoionization cross-sections has the true threshold behavior while recombination cross-sections can be recalculated using the corresponding relations presented in [6]. The approach developed provides a useful tool for calculations of threshold phenomena in the formation and ionization of (anti)hydrogen-like atoms and ions in magnetic traps.

Acknowledgements

The authors thank Prof. V.L. Derbov for a long-time collaboration. O.C. and M.S.K. acknowledge financial support from a grant of the President of the Bulgarian Fund for Scientific Investigations under grant I-1402/2004-2007 and the theme 09-6-1060-2005/2009 “Mathematical support of experimental and theoretical studies conducted by JINR”. V.P.G. and A.A.G. acknowledge partial support from the Russian Foundation for Basic Research under grant No. 07-01-00660.

Appendix A

```
****** BEGIN OF THE POTHMF RUN ******

PROBLEM:      Potential and dipole matrices elements
********


                C O N T R O L   I N F O R M A T I O N
                -------------------------------------
```

```
   NUMBER OF DIFFERENTIAL EQUATIONS. . . . . (MDIM  ) =      6
   ORDER OF SHAPE FUNCTIONS. . . . . . . . . (NPOL  ) =      4
   ORDER OF GAUSS-LEGENDRE QUADRATURE. . . . (NGQ   ) =      5
   VALUE OF NUCLEAR CHARGE . . . . . . . . . (CHARGE) =    1.00000
   VALUE OF CYCLOTRON FREQUENCY. . . . . . . (WC    ) =    1.00000
   VALUE OF THE RELATIVE MACHINE PRECISION . (EPSY  ) =   0.222045E-15

            SPECIFICATIONS OF THE FIRST ATOMIC STATE
            ---------------------------------------

   NUMBER OF FINITE ELEMENTS . . . . . . . . (NELEM ) =    600
   NUMBER OF GRID POINTS . . . . . . . . . . (NGRID ) =   2401
   PARITY OF STATE . . . . . . . . . . . . . (IPARTL) =      1
   MAGNETIC QUANTUM NUMBER . . . . . . . . . (MQNL  ) =      0
   VALUE OF MATCHING POINT FOR EPSY. . . . . (RMATCH) =    39.0953

  SUBDIVISION OF RHO-REGION ON THE FINITE-ELEMENT GROUPS:
  ******************************************************

 NO OF  NUMBER OF  BEGIN OF  LENGTH OF    GRID     END OF
 GROUP  ELEMENTS   INTERVAL   ELEMENT     STEP    INTERVAL
 -----  ---------  --------  ---------  --------  --------
   1       200        0.000   0.01500   0.00375      3.000
   2       200        3.000   0.08500   0.02125     20.000
   3       200       20.000   0.40000   0.10000    100.000

   LAST ADDRESS OF ARRAY ITOT USED =       3763

   LAST ADDRESS OF ARRAY TOT USED =       9728


        POTENTIAL MATRICES V(I,J) AND Q(I,J):

   V-MATRIX AT THE POINT NO =     1  AND RADIUS RHO =     0.00070
0.4037D+07  0.1102D-37  -.4472D-22  -.1240D-37  -.5652D-53  -.8437D-69
0.1102D-37  0.2423D+08  0.2229D-37  -.1652D-22  -.5592D-38  -.9780D-54
-.4472D-22  0.2229D-37  0.6059D+08  0.7030D-38  -.8664D-23  -.2173D-38
-.1240D-37  -.1652D-22  0.7030D-38  0.1131D+09  0.3990D-38  -.5343D-23
-.5652D-53  -.5592D-38  -.8664D-23  0.3990D-38  0.1818D+09  -.4761D-39
-.8437D-69  -.9780D-54  -.2173D-38  -.5343D-23  -.4761D-39  0.2666D+09

   Q-MATRIX AT THE POINT NO =     1  AND RADIUS RHO =     0.00070
0.0000D+00  0.9123D-11  0.2248D-26  0.2423D-42  0.2522D-57  -.6243D-73
-.9123D-11  0.0000D+00  0.4902D-11  0.5284D-27  0.3385D-42  -.8045D-58
-.2248D-26  -.4902D-11  0.0000D+00  0.3370D-11  0.8637D-27  -.1858D-42
-.2423D-42  -.5284D-27  -.3370D-11  0.0000D+00  0.2571D-11  -.4205D-27
-.2522D-57  -.3385D-42  -.8637D-27  -.2571D-11  0.0000D+00  0.2079D-11
0.6243D-73  0.8045D-58  0.1858D-42  0.4205D-27  -.2079D-11  0.0000D+00


        POTENTIAL MATRICES V(I,J) AND Q(I,J):

   V-MATRIX AT THE POINT NO =  1502  AND RADIUS RHO =    11.51962
0.8265D+00  0.1209D-03  -.1543D-01  -.3686D-03  -.9037D-05  -.2528D-06
0.1209D-03  0.2827D+01  0.6268D-03  -.4704D-01  -.1537D-02  -.4837D-04
-.1543D-01  0.6268D-03  0.4829D+01  0.1953D-02  -.9569D-01  -.4014D-02
-.3686D-03  -.4704D-01  0.1953D-02  0.6833D+01  0.4612D-02  -.1623D+00
-.9037D-05  -.1537D-02  -.9569D-01  0.4612D-02  0.8840D+01  0.9217D-02
-.2528D-06  -.4837D-04  -.4014D-02  -.1623D+00  0.9217D-02  0.1085D+02

   Q-MATRIX AT THE POINT NO =  1502  AND RADIUS RHO =    11.51962
0.0000D+00  0.8748D-01  0.6854D-03  0.8256D-05  0.1360D-06  0.2879D-08
```

```
-.8748D-01  0.0000D+00  0.1764D+00  0.2124D-02  0.3501D-04  0.7408D-06
-.6854D-03  -.1764D+00  0.0000D+00  0.2668D+00  0.4396D-02  0.9302D-04
-.8256D-05  -.2124D-02  -.2668D+00  0.0000D+00  0.3589D+00  0.7592D-02
-.1360D-06  -.3501D-04  -.4396D-02  -.3589D+00  0.0000D+00  0.4528D+00
-.2879D-08  -.7408D-06  -.9302D-04  -.7592D-02  -.4528D+00  0.0000D+00

             SPECIFICATIONS OF THE SECOND ATOMIC STATE
             -----------------------------------------

   NUMBER OF FINITE ELEMENTS . . . . . (NELEM ) =    600
   NUMBER OF GRID POINTS . . . . . (NGRID ) =   2401
   PARITY OF STATE . . . . . (IPARTR) =      0
   MAGNETIC QUANTUM NUMBER . . . . . (MQNR  ) =      0
   VALUE OF MATCHING POINT FOR EPSY. . . . . (RMATCH) =    39.0953

  SUBDIVISION OF RHO-REGION ON THE FINITE-ELEMENT GROUPS:
  ******************************************************

 NO OF  NUMBER OF  BEGIN OF  LENGTH OF    GRID     END OF
 GROUP  ELEMENTS   INTERVAL   ELEMENT     STEP    INTERVAL
 -----  ---------  --------  ---------  --------  --------
   1       200        0.000   0.01500   0.00375      3.000
   2       200        3.000   0.08500   0.02125     20.000
   3       200       20.000   0.40000   0.10000    100.000

   LAST ADDRESS OF ARRAY ITOT USED =       3773

   LAST ADDRESS OF ARRAY TOT USED =       9773


         POTENTIAL MATRICES V(I,J) AND Q(I,J):

   V-MATRIX AT THE POINT NO =     1  AND RADIUS RHO =     0.00070
-.2842D+04  0.4927D-37  -.1101D-21  -.4812D-37  -.7324D-53  -.4207D-68
0.4927D-37  0.1212D+08  0.1381D-36  -.2539D-22  -.4899D-38  -.2117D-53
-.1101D-21  0.1381D-36  0.4039D+08  0.7232D-38  -.1164D-22  -.3356D-38
-.4812D-37  -.2539D-22  0.7232D-38  0.8482D+08  0.4288D-38  -.6703D-23
-.7324D-53  -.4899D-38  -.1164D-22  0.4288D-38  0.1454D+09  0.2719D-38
-.4207D-68  -.2117D-53  -.3356D-38  -.6703D-23  0.2719D-38  0.2222D+09

   Q-MATRIX AT THE POINT NO =     1  AND RADIUS RHO =     0.00070
0.0000D+00  0.1731D-10  0.7747D-26  0.1209D-41  0.1293D-57  0.1062D-65
-.1731D-10  0.0000D+00  0.6359D-11  0.9926D-27  0.7835D-43  0.9405D-58
-.7747D-26  -.6359D-11  0.0000D+00  0.3993D-11  0.3152D-27  0.2018D-42
-.1209D-41  -.9926D-27  -.3993D-11  0.0000D+00  0.2916D-11  0.6590D-27
-.1293D-57  -.7835D-43  -.3152D-27  -.2916D-11  0.0000D+00  0.2298D-11
-.1062D-65  -.9405D-58  -.2018D-42  -.6590D-27  -.2298D-11  0.0000D+00


         POTENTIAL MATRICES V(I,J) AND Q(I,J):

   V-MATRIX AT THE POINT NO =  1502  AND RADIUS RHO =    11.51962
0.8265D+00  0.1209D-03  -.1543D-01  -.3686D-03  -.9037D-05  -.2528D-06
0.1209D-03  0.2827D+01  0.6268D-03  -.4704D-01  -.1537D-02  -.4837D-04
-.1543D-01  0.6268D-03  0.4829D+01  0.1953D-02  -.9569D-01  -.4014D-02
-.3686D-03  -.4704D-01  0.1953D-02  0.6833D+01  0.4612D-02  -.1623D+00
-.9037D-05  -.1537D-02  -.9569D-01  0.4612D-02  0.8840D+01  0.9217D-02
-.2528D-06  -.4837D-04  -.4014D-02  -.1623D+00  0.9217D-02  0.1085D+02

   Q-MATRIX AT THE POINT NO =  1502  AND RADIUS RHO =    11.51962
0.0000D+00  0.8748D-01  0.6854D-03  0.8256D-05  0.1360D-06  0.2879D-08
-.8748D-01  0.0000D+00  0.1764D+00  0.2124D-02  0.3501D-04  0.7408D-06
```

```
-.6854D-03  -.1764D+00  0.0000D+00  0.2668D+00  0.4396D-02  0.9302D-04
-.8256D-05  -.2124D-02  -.2668D+00  0.0000D+00  0.3589D+00  0.7592D-02
-.1360D-06  -.3501D-04  -.4396D-02  -.3589D+00  0.0000D+00  0.4528D+00
-.2879D-08  -.7408D-06  -.9302D-04  -.7592D-02  -.4528D+00  0.0000D+00

             SPECIFICATIONS OF THE DIPOLE MATRICES
             -------------------------------------

   NUMBER OF FINITE ELEMENTS . . . . . (NELEM ) =    600
   NUMBER OF GRID POINTS . . . . . (NGRID ) =   2401
   PARITY OF STATE . . . . . (IPARTL) =      1
   MAGNETIC QUANTUM NUMBER . . . . . (MQNL  ) =      0
   PARITY OF STATE . . . . . (IPARTR) =      0
   MAGNETIC QUANTUM NUMBER . . . . . (MQNR  ) =      0
   VALUE OF MATCHING POINT FOR EPSY. . . . . (RMATCH) =    41.4000

  SUBDIVISION OF RHO-REGION ON THE FINITE-ELEMENT GROUPS:
  ******************************************************

 NO OF  NUMBER OF  BEGIN OF  LENGTH OF    GRID     END OF
 GROUP  ELEMENTS   INTERVAL   ELEMENT     STEP    INTERVAL
 -----  ---------  --------  ---------  --------  --------
   1       200        0.000   0.01500   0.00375      3.000
   2       200        3.000   0.08500   0.02125     20.000
   3       200       20.000   0.40000   0.10000    100.000

   LAST ADDRESS OF ARRAY ITOT USED =       3419

   LAST ADDRESS OF ARRAY TOT USED =       9293


        DIPOLE MATRICES D(I,J):

   D-MATRIX AT THE POINT NO =     1  AND RADIUS RHO =     0.00000
0.0000D+00  0.0000D+00  0.0000D+00  0.0000D+00  0.0000D+00  0.0000D+00
0.0000D+00  0.0000D+00  0.0000D+00  0.0000D+00  0.0000D+00  0.0000D+00
0.0000D+00  0.0000D+00  0.0000D+00  0.0000D+00  0.0000D+00  0.0000D+00
0.0000D+00  0.0000D+00  0.0000D+00  0.0000D+00  0.0000D+00  0.0000D+00
0.0000D+00  0.0000D+00  0.0000D+00  0.0000D+00  0.0000D+00  0.0000D+00
0.0000D+00  0.0000D+00  0.0000D+00  0.0000D+00  0.0000D+00  0.0000D+00


        DIPOLE MATRICES D(I,J):

   D-MATRIX AT THE POINT NO =  1502  AND RADIUS RHO =    17.89625
0.1784D+02  0.5605D-01  0.1778D-03  0.8543D-06  0.5527D-08  0.4514D-10
0.5605D-01  0.1773D+02  0.1125D+00  0.5403D-03  0.3496D-05  0.2855D-07
0.1778D-03  0.1125D+00  0.1761D+02  0.1692D+00  0.1095D-02  0.8944D-05
0.8543D-06  0.5403D-03  0.1692D+00  0.1750D+02  0.2264D+00  0.1849D-02
0.5527D-08  0.3496D-05  0.1095D-02  0.2264D+00  0.1738D+02  0.2839D+00
0.4514D-10  0.2855D-07  0.8944D-05  0.1849D-02  0.2839D+00  0.1726D+02

             SPECIFICATIONS OF THE ASYMPTOTIC SOLUTION
             -----------------------------------------

   NUMBER OF DIFFERENTIAL EQUATIONS. . . . . (MDIM  ) =      6
   NUMBER OF OPEN CHANNEL. . . . . (NOPEN ) =      2
   ORDER OF CALCULATION. . . . . (IFUNAS) =     15
   PARITY OF STATE . . . . . (IPARTL) =      1
   MAGNETIC QUANTUM NUMBER . . . . . (MQNL  ) =      0
   CHARGE OF NUCLEAR . . . . . (CHARGE) =    1.00000
   MAGNETIC PARAMETER. . . . . (WC    ) =    1.00000
```

```
    DOUBLE ENERGY SPECTRUM. . . . . . . . . . (SHIFT ) =    3.40000
    VALUE OF CALCULATED POINT . . . . . . . . (RMAX  ) =    100.000

    LAST ADDRESS OF ARRAY TOT USED =       1166

    VALUE OF I-TH THRESHOLD ENERGY (IN RY). (I,THR) =      1  0.1000E+01
    VALUE OF I-TH THRESHOLD ENERGY (IN RY). (I,THR) =      2  0.3000E+01
    VALUE OF I-TH MOMENTUM. . . . . . . . . (I,QR ) =      1  0.1549E+01
    VALUE OF I-TH MOMENTUM. . . . . . . . . (I,QR ) =      2  0.6325E+00


    TO HAVE REQUIRED EPSC=1.D-14
    VALUE OF MATCHING POINT   (RMATCH) =   31.6417
    RECOMMENDED RIGHT BOUND OF
    INTERVAL IS NOT LESS THAN (RMAX  ) =   33


          CHECK WRONSKIAN
         -----------------
 1.00000     -.102478E-17
0.197052E-17  1.00000

          REGULAR SOLUTIONS
         -------------------
0.778672E-02 -.277717E-04
-.281771E-04 0.117197E-01
-.150402E-05 -.535513E-04
0.243486E-08 0.289640E-06
-.518989E-10 -.109459E-07
0.515806E-12 -.195459E-09

          IRREGULAR SOLUTIONS
         ---------------------
-.190795E-02 -.755766E-04
-.121508E-03 -.411903E-02
0.331762E-06 -.151932E-03
0.112340E-07 -.725747E-07
0.699426E-11 -.330613E-07
0.307317E-11 0.718648E-10

          DERIVATIVE OF REGULAR SOLUTIONS
         ---------------------------------
-.304607E-02 -.484243E-04
-.188492E-03 -.278605E-02
0.561492E-06 -.974143E-04
0.173828E-07 -.550720E-07
0.134532E-10 -.210016E-07
0.475254E-11 0.566044E-10

          DERIVATIVE OF IRREGULAR SOLUTIONS
         -----------------------------------
-.120955E-01 0.195204E-04
0.462741E-04 -.755679E-02
0.233031E-05 0.377738E-04
-.424123E-08 -.186102E-06
0.804558E-10 0.841921E-08
-.987484E-12 0.123011E-09

******   END OF THE POTHMF RUN ******

****** BEGIN OF THE KANTBP RUN ******
```

```
 PROBLEM:     Bound state energy levels
 ********

              C O N T R O L  I N F O R M A T I O N
              -----------------------------------

    NUMBER OF DIFFERENTIAL EQUATIONS. . . . . (MDIM  ) =      6
    NUMBER OF ENERGY LEVELS REQUIRED. . . . . (NROOT ) =      1
    NUMBER OF FINITE ELEMENTS . . . . . . . . (NELEM ) =    600
    NUMBER OF GRID POINTS . . . . . . . . . . (NGRID ) =   2401
    ORDER  OF SHAPE FUNCTIONS . . . . . . . . (NPOL  ) =      4
    ORDER  OF GAUSS-LEGENDRE QUADRATURE . . . (NGQ   ) =      5
    NUMBER OF SUBSPACE ITERATION VECTORS. . . (NC    ) =      2
    DIMENSION OF ENVELOPE SPACE . . . . . . . (IDIM  ) =      3
    BOUNDARY CONDITION CODE . . . . . . . . . (IBOUND) =      3
    SHIFT OF DOUBLE ENERGY SPECTRUM . . . . . (SHIFT ) =  -0.700000
    CONVERGENCE TOLERANCE . . . . . . . . . . (RTOL  ) =   0.100000E-14


   SUBDIVISION OF RHO-REGION ON THE FINITE-ELEMENT GROUPS:
   ******************************************************

  NO OF  NUMBER OF  BEGIN OF  LENGTH OF    GRID     END OF
  GROUP  ELEMENTS   INTERVAL   ELEMENT     STEP    INTERVAL
  -----  ---------  --------  ---------  --------  --------
    1       200        0.000   0.01500   0.00375      3.000
    2       200        3.000   0.08500   0.02125     20.000
    3       200       20.000   0.40000   0.10000    100.000

    LAST ADDRESS OF ARRAY ITOT USED =      64222


              T O T A L  S Y S T E M  D A T A
              -------------------------------

    TOTAL NUMBER OF ALGEBRAIC EQUATIONS. . . (NN ) =    14400
    TOTAL NUMBER OF MATRIX ELEMENTS. . . . . (NWK) =   266256
    MAXIMUM HALF BANDWIDTH . . . . . . . . . (MK ) =       30
    MEAN    HALF BANDWIDTH . . . . . . . . . (MMK) =       18


    LAST ADDRESS OF ARRAY TOT USED =     538201


    NDIM, MDIM=         6         6


    LAST ADDRESS OF ARRAY TOT USED =     593029

 THERE ARE    0 ROOTS LOWER THEN SHIFT
 CONVERGENCE REACHED FOR RTOL 0.1000E-14
 I T E R A T I O N   N U M B E R    9
 RELATIVE TOLERANCE REACHED ON EIGENVALUES
  0.1781E-15

*******************************************************************************


   R O O T   N U M B E R     E I G E N V A L U E
  ----------------------   --------------------
            1               -0.3311688955144392
```

```
*******************************************************************************
       R       R A D I A L   E I G E N F U N C T I O N S
       -       ----------------------------------------

     0.0000  0.2406D+01 0.2984D-12 -.4758D-15 0.6931D-18 0.3585D-23 0.2470D-28
     1.8000  0.3050D+00 -.1487D-01 0.5042D-03 0.1610D-04 0.4848D-06 0.1190D-07
     6.4000  0.3819D-03 -.8983D-04 0.2920D-04 -.1130D-04 0.4997D-05 -.3193D-05
    16.6000  0.5146D-09 -.4291D-10 0.4720D-11 -.5886D-12 0.8179D-13 -.1266D-13
    52.0000  0.7291D-15 0.6787D-18 0.1469D-18 0.1157D-20 0.1846D-21 0.1947D-22

*******************************************************************************

 PROBLEM:     Reaction matrix
 ********


              C O N T R O L  I N F O R M A T I O N
              -----------------------------------

    NUMBER OF DIFFERENTIAL EQUATIONS. . . . . (MDIM  ) =      6
    NUMBER OF FINITE ELEMENTS . . . . . . . . (NELEM ) =    600
    NUMBER OF GRID POINTS . . . . . . . . . . (NGRID ) =   2401
    ORDER OF SHAPE FUNCTIONS. . . . . . . . . (NPOL  ) =      4
    ORDER OF GAUSS-LEGENDRE QUADRATURE. . . . (NGQ   ) =      5
    DIMENSION OF ENVELOPE SPACE . . . . . . . (IDIM  ) =      3
    BOUNDARY CONDITION CODE . . . . . . . . . (IBOUND) =      8
    DOUBLE ENERGY SPECTRUM. . . . . . . . . . (SHIFT ) =    3.40000


   SUBDIVISION OF RHO-REGION ON THE FINITE-ELEMENT GROUPS:
   ******************************************************

  NO OF  NUMBER OF  BEGIN OF  LENGTH OF    GRID     END OF
  GROUP  ELEMENTS   INTERVAL   ELEMENT     STEP    INTERVAL
  -----  ---------  --------  ---------  --------  --------
    1       200        0.000   0.01500   0.00375      3.000
    2       200        3.000   0.08500   0.02125     20.000
    3       200       20.000   0.40000   0.10000    100.000

    LAST ADDRESS OF ARRAY ITOT USED =      64222


              T O T A L  S Y S T E M  D A T A
              -------------------------------

    TOTAL NUMBER OF ALGEBRAIC EQUATIONS. . . (NN ) =    14406
    TOTAL NUMBER OF MATRIX ELEMENTS. . . . . (NWK) =   266421
    MAXIMUM HALF BANDWIDTH . . . . . . . . . (MK ) =       30
    MEAN    HALF BANDWIDTH . . . . . . . . . (MMK) =       18


    LAST ADDRESS OF ARRAY TOT USED =     272110


    NDIM, MDIM=         6         6


    LAST ADDRESS OF ARRAY TOT USED =     384669

    NUMBER OF OPEN CHANNELS. . . . . . . . . (NOPEN) =      2
    VALUE OF I-TH MOMENTUM . . . . . . . . . (I,QR ) =      1  0.1549E+01
    VALUE OF I-TH MOMENTUM . . . . . . . . . (I,QR ) =      2  0.6325E+00
```

```
     TO HAVE REQUIRED EPSC=1.D-14
     VALUE OF MATCHING POINT   (RMATCH) =   31.6417
     RECOMMENDED RIGHT BOUND OF
     INTERVAL IS NOT LESS THAN (RMAX  ) =   33

          C H E C K  W R O N S K I A N
         ------------------------------
  1.00000     -.102478E-17
 0.197052E-17  1.00000

*******************************************************************************

          R E A C T I O N   M A T R I X
         ------------------------------
 -1.46347      2.19626
  2.19626     -8.72933

*******************************************************************************


       R        R A D I A L   E I G E N F U N C T I O N S
       -        ---------------------------------------

    0.0000  0.6464D-13 0.1723D-11 0.4879D-12 -.1955D-11 -.3150D-13 0.7927D-13
            0.6148D-18 -.2533D-17 0.1684D-22 -.6326D-22 0.4306D-27 -.1633D-26
    1.8000  -.2666D-01 0.6352D+00 -.8888D+00 0.2455D+01 0.1111D-01 -.4781D-01
            0.4547D-02 -.1653D-01 0.3372D-03 -.1260D-02 0.1491D-04 -.5729D-04
    6.4000  -.2597D+00 0.4054D+00 0.1543D+00 -.4776D+00 -.8057D-01 0.3852D+00
            -.3576D-02 0.1317D-01 -.1418D-02 0.7051D-02 -.1987D-02 0.7691D-02
   16.6000  0.5866D-01 -.1008D+00 -.1550D+00 0.6160D+00 -.4496D-02 0.1061D-01
            0.9199D-04 -.2742D-03 -.4298D-04 0.1278D-03 0.6092D-05 -.2478D-04
   52.0000  0.2643D-01 -.2289D-01 -.1825D-01 0.9443D-01 -.1258D-02 0.4726D-02
            -.5400D-06 0.3805D-05 -.9910D-06 0.3781D-05 0.4891D-08 -.2518D-07
  100.0000  0.1041D-01 -.3558D-02 -.8897D-02 0.4741D-01 -.3357D-03 0.1273D-02
            -.1734D-06 0.9478D-06 -.7267D-07 0.2777D-06 0.1539D-09 -.8160D-09

*******************************************************************************

 ******   END OF THE KANTBP RUN ******
```

References

[1] J.I. Kim, V.S. Melezhik, P. Schmelcher, Phys. Rev. Lett. 97 (2006) 193203-1–4.
[2] Yu.N. Demkov, J.D. Meyer, Eur. Phys. J. B 42 (2004) 361–365.
[3] A. Wetzels, A. Gurtler, L.D. Noordam, F. Robicheaux, Phys. Rev. A 73 (2006) 062507-1–8.
[4] A. Rotondi, M. Amoretti, et al., AIP Conference Proceedings 796 (2005) 285–290.
[5] M.V. Ryabinina, L.A. Melnikov, Nuclear Instruments and Methods in Physics Research Section B 214 (2004) 35–39;
M.V. Ryabinina, L.A. Melnikov, AIP Conference Proceedings 796 (2005) 325–329.
[6] V.V. Serov, V.L. Derbov, S.I. Vinitsky, Optics and Spectroscopy 102 (2007) 557–561.
[7] A.G. Abrashkevich, M. Shapiro, Phys. Rev. A 50 (1994) 1205–1217;
A.G. Abrashkevich, M. Shapiro, J. Phys. B 29 (1996) 627–644.
[8] M.S. Kaschiev, S.I. Vinitsky, F.R. Vukajlovic, Phys. Rev. A 22 (1980) 557–559.
[9] A.G. Abrashkevich, D.G. Abrashkevich, M. Shapiro, Comput. Phys. Comm. 90 (1995) 311–339.
[10] M.G. Dimova, M.S. Kaschiev, S.I. Vinitsky, J. Phys. B 38 (2005) 2337–2352.
[11] A. Alijah, J. Hinze, J.T. Broad, J. Phys. B 23 (1990) 45–60.
[12] Q. Wang, C.H. Greene, Phys. Rev. A 44 (1991) 7448–7458.
[13] U. Fano, E.Y. Sidky, Phys. Rev. A 45 (1992) 4776–4791;
E.Y. Sidky, Phys. Rev. A 47 (1993) 2812–2818.
[14] S. Watanabe, H.-A. Komine, Phys. Rev. Lett. 67 (1991) 3227–3230.
[15] D. Delande, A. Bommier, J.C. Gay, Phys. Rev. Lett. 66 (1991) 141–144.
[16] N. Merani, J. Main, G. Wunner, Astron. Astrophys. 298 (1995) 193–203.
[17] L.B. Zhao, P.C. Stancil, Phys. Rev. A 74 (2006) 055401-1–4.
[18] J. Eichler, Y. Yoshihama, N. Toshima, Phys. Rev. A 65 (2002) 033404-1–6.

[19] C.V. Clark, K.T. Lu, A.F. Starace, in: H.G. Beyer, H. Kleinpoppen (Eds.), Progress in Atomic Spectroscopy, Part C, Plenum, New York, 1984, pp. 247–320.
[20] O. Chuluunbaatar, A.A. Gusev, V.L. Derbov, M.S. Kaschiev, V.V. Serov, T.V. Tupikova, S.I. Vinitsky, Proc. SPIE 6165 (2006) 61650B-1–17.
[21] L.V. Kantorovich, V.I. Krylov, Approximate Methods of Higher Analysis, Wiley, New York, 1964.
[22] M. Abramovits, I.A. Stegun, Handbook of Mathematical Functions, Dover, New York, 1965.
[23] S.I. Vinitsky, V.P. Gerdt, A.A. Gusev, M.S. Kaschiev, V.A. Rostovtsev, V.N. Samoylov, T.V. Tupikova, O. Chuluunbaatar, Programming and Computer Software 33 (2007) 105–116.
[24] J.D. Power, Phil. Trans. Roy. Soc. London A 274 (1973) 663–702.
[25] J.H. Wilkinson, Lin. Algebra Appl. 1 (1968) 409–420.
[26] O. Chuluunbaatar, A.A. Gusev, A.G. Abrashkevich, A. Amaya-Tapia, M.S. Kaschiev, S.Y. Larsen, S.I. Vinitsky, Comput. Phys. Comm. 177 (2007) 649–675.
[27] M.J. Seaton, Rep. Prog. Phys. 46 (1983) 167–257.
[28] O. Chuluunbaatar, A.A. Gusev, V.L. Derbov, M.S. Kaschiev, V.V. Serov, T.V. Tupikova, S.I. Vinitsky, Proc. SPIE 6537 (2007) 653706-1–18.
[29] O. Chuluunbaatar, A.A. Gusev, V.L. Derbov, M.S. Kaschiev, L.A. Melnikov, V.V. Serov, S.I. Vinitsky, J. Phys. A 40 (2007) 11485–11524.
[30] U. Fano, C.M. Lee, Phys. Rev. Lett. 31 (1973) 1573–1576.
[31] C.M. Lee, Phys. Rev. A 10 (1974) 584–600.
[32] A.G. Abrashkevich, M.S. Kaschiev, S.I. Vinitsky, J. Comp. Phys. 163 (2000) 328–348.
[33] http://www.netlib.org/lapack/.
[34] A.A. Gusev, V.P. Gerdt, M.S. Kaschiev, V.A. Rostovtsev, V.N. Samoylov, T.V. Tupikova, S.I. Vinitsky, in: Lecture Notes in Computer Science, vol. 4194, 2006, pp. 205–218.
[35] T. Oguchi, Radio Sci. 5 (1970) 1207–1214.
[36] S.L. Skorokhodov, D.V. Khristoforov, Comp. Math. Math. Phys. 46 (2006) 1132–1146.
[37] R.J. Damburg, R.Kh. Propin, J. Phys. B 1 (1968) 681–691.
[38] M. Gailitis, J. Phys. B 9 (1976) 843–854.
[39] W.H. Press, S.A. Teukolsky, W.T. Vetterling, B.P. Flannery, Numerical Recipes: The Art of Scientific Computing, Cambridge University Press, Cambridge, 1986.
[40] A.R. Barnett, D.H. Feng, J.W. Steed, L.J.B. Goldfarb, Comput. Phys. Comm. 8 (1974) 377–395.
[41] http://physics.nist.gov/cuu/Constants/index.html.